applied sciences

MDPI

Article

Evaluation and Comparison of Meteorological Measurements by a UAS with High-Resolution Numerical Weather Prediction Simulations

Wai Hung Leung, Ming Chun Lam, Kai Kwong Lai and Pak Wai Chan *

Hong Kong Observatory, Hong Kong, China; whleung@hko.gov.hk (W.H.L.)
* Correspondence: pwchan@hko.gov.hk

Abstract

The performance of the meteorological measurements of an Unmanned Aircraft System (UAS) is studied in this paper by comparison with the simultaneous data collected by a wind mast, a radiosonde sensing package and ground-based, remote-sensing meteorological instruments at the radiosonde station of King's Park, Hong Kong. They are found to meet the "breakthrough" level requirement of the World Meteorological Organization. The UAS is then used to collect meteorological data for the first time at a sandbox project location in Hong Kong for low altitude economy (LAE), namely, an area of complex terrain at an isolated island called Peng Chau. Some interesting features are identified in the vertical profiling flight of wind speed and turbulent kinetic energy (TKE), which forms the basis for developing meteorological support for LAE at this site in the future. High-resolution numerical weather prediction (NWP) simulation is then performed and evaluated statistically by comparison with UAS measurements at these two locations. The simulation of wind direction and TKE appears to be rather challenging as demonstrated in this comparison exercise. The root-mean-square-error of the simulated TKE is found to be of a similar order of magnitude as the absolute value itself, and the wind direction from the outer domain is found to have limited "correction" with the use of high-resolution terrain data in the NWP simulation with the mesoscale model. Further research directions for the simulation are discussed, with the objective of providing weather forecasting services for supporting LAE developments in Hong Kong.

Keywords: Unmanned Aircraft System; low altitude economy; numerical weather prediction

1. Introduction

Meteorological measurements by Unmanned Aircraft Systems (UAS) is a hot topic in many parts of the world as the data collected are crucial for supporting the activities of low altitude economy (LAE), which refers to economic activities in airspace below 1000 m that presents a wide array of application scenarios including rescues, surveys and delivery of goods and passengers [1–3], where representativeness of UAS sampling within the convective boundary layer has been quantified recently [4]. In Hong Kong, for LAE developments, a number of sandbox projects have been identified and it is important to carry out meteorological measurements at the potential flight routes, including the use of UAS, micro-climate station near the ground, and ground-based remote-sensing meteorological measuring systems such as Doppler Light Detection and Ranging (LIDAR) system and microwave wind radar, in order to understand more about the weather conditions at the localized areas for providing weather support services for the sandbox projects [5].

Check for updates

Academic Editor: Rosario Pecora

Received: 24 February 2026
Revised: 27 April 2026
Accepted: 26 May 2026
Published: 2 June 2026

Copyright: © 2026 by the authors. Licensee MDPI, Basel, Switzerland. This article is an open access article distributed under the terms and conditions of the Creative Commons Attribution (CC BY) license.

UAS-based atmospheric measurements have advanced considerably in recent years, with international efforts such as the LAPSE-RATE campaign establishing intercomparison standards for small UAS platforms used in atmospheric science [6]. Studies have demonstrated their utility for boundary layer characterization, though challenges remain in complex terrain and urban environments where terrain-induced flow features and urban parameterization introduce significant uncertainties. For LAE applications, meteorological support requirements differ from conventional aviation due to lower operating altitudes where conventional observation networks provide limited coverage. In Hong Kong, previous work has examined urban wind characteristics using microclimate stations and high-resolution numerical simulations [7], but systematic evaluation of UAS measurements against high-resolution NWP simulations at LAE sandbox locations remains limited, particularly for turbulence parameters critical for flight safety.

In this paper, the quality of the weather data collected by a UAS is firstly evaluated by comparison with the existing meteorological measurements, including point measurement by a wind mast (anemometer), vertical wind profiling by ground-based remote-sensing instruments, and a radiosonde attached to the aircraft. Then, meteorological measurements are performed at a sandbox project location for the first time, namely, Peng Chau (a small island in the central waters of Hong Kong, between the Hong Kong Island and Lantau Island), in order to capture specific features of the wind at that localized area. The weather data collected by the UAS are also compared with the simulation results by a high-resolution numerical weather prediction (NWP) model, with particular interest in the low-level turbulence expressed in terms of the turbulent kinetic energy (TKE). Some features of the airflow at Peng Chau are also studied using the NWP model.

The novelty of this work lies in several key contributions. First, we provide a rigorous multi-instrument validation of the UAS meteorological sensors against four independent reference systems (wind mast, radiosonde, LIDAR, and microwave radar), demonstrating compliance with WMO 'breakthrough' level requirements. Second, we systematically evaluate high-resolution (40 m) NWP model performance against UAS measurements at two distinct environments (urban and complex terrain), identifying specific challenges in wind direction and turbulent kinetic energy simulation that have direct implications for LAE weather support services. The results in this paper showcase (a) a comprehensive evaluation of UAS meteorological measurements, and (b) the comparison of UAS-measured meteorological data with NWP simulations of the meteorological conditions at a sandbox project location in Hong Kong. The methods established in this paper would form the basis for the future, more widespread use of UAS for meteorological measurements in Hong Kong and the study of the meteorological conditions at the tens of sandbox project locations within the territory. This work addresses a critical knowledge gap in understanding the atmospheric conditions at low altitudes where LAE operations will occur, particularly in the complex terrain and urban environments characteristic of the Hong Kong region [7]. The results would also serve as a useful reference for LAE projects in other parts of the world.

2. UAS Measurements Methodology and Results

The UAS in use is manufactured by DJI, model M350 RTK. The dimensions unfolded (not including rotors) are 810 mm × 670 mm × 430 mm (length, width and height). The weight of the UAS itself is 6.47 kg, with a maximum payload of 2.73 kg. The maximum wind speed resistance is 12 m/s and the maximum flight time is 55 min. The global navigation satellite system (GNSS) used in the UAS includes GPS, GLONASS, Beidou and Galileo. There are two sets of meteorological sensors:

(a) Temperature and relative humidity sensor—manufactured by Vaisala, model HMP110, measuring temperature and relative humidity with a weight of 17 g;

(b) Wind speed and direction sensing module—sonic anemometer manufactured by LI-COR, model LI-550, measuring horizontal wind speed and wind direction, with a weight of 60 g.

Details of the meteorological sensors is provided in Table 1. A photo of the UAS mounted with meteorological equipment is shown in Figure 1 (right panel). The data, available in 1 Hz, were stored and processed by a unit manufactured by Soarability, model Sniffer4D Mini2.

Table 1. The parameter, range, accuracy, resolution and response time of the meteorological sensors used on the UAS.

Sensor	Parameter	Range	Accuracy	Resolution	Response Time
Vaisala HMP110	Temperature	−40 to 80 °C	±0.1 to ±0.4 °C	/	/
	Relative Humidity	0 to 100%	±1.1 to ±4.0%	/	60 s
LI-COR LI-550	Wind Speed	0 to 50 m/s	±0.2 m/s to ±4%	0.01 m/s	/
	Wind Direction	0–359°	±1.0°	1.0°	/
Vaisala RS41-SG	Temperature	−95 to 60 °C	±0.1 to 0.4 °C	0.01 °C	0.5 s
	Relative Humidity	0 to 100%	±2 to 4%	0.1%	0.3 to 10 s

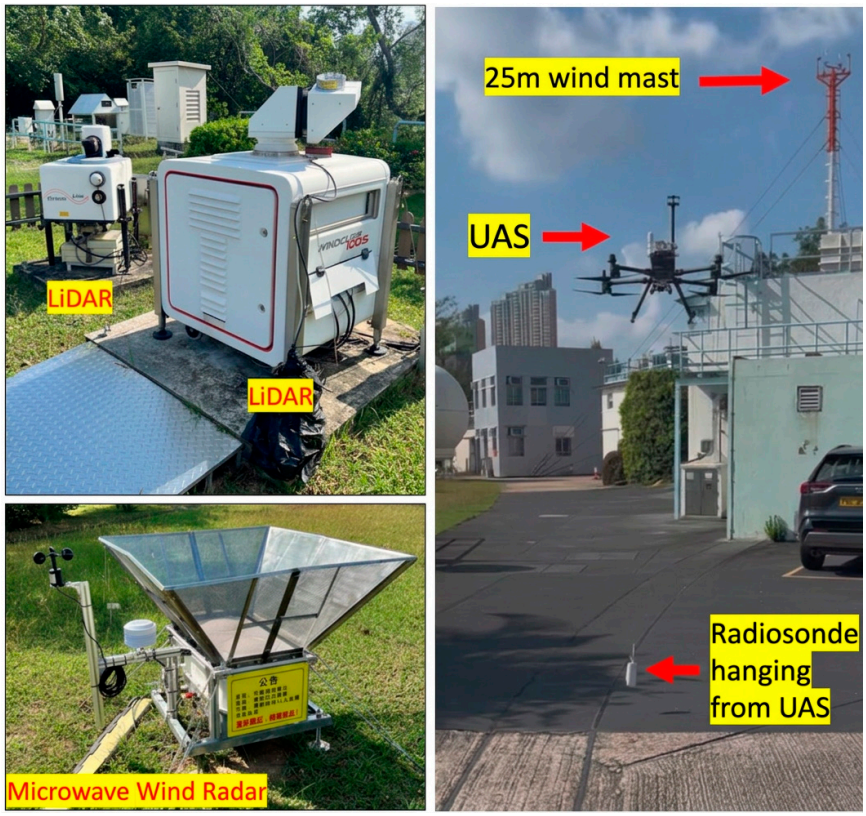


Figure 1. The UAS in use (**right-hand side**) with the wind mast nearby and the attached radiosonde. The ground-based, remote-sensing instruments in use are shown on the (**left-hand side**), including LIDARs and microwave wind radar.

2.1. UAS Measurement Methodology and Results at King's Park Meteorological Station

In order to evaluate the performance of meteorological measurements with the UAS, the collected weather data were compared with the simultaneous data measured by other weather instruments at the radiosonde station in Hong Kong, namely, King's Park in the urban area of Kowloon, including a wind mast, ground-based LIDARs that measure the three components of the wind by Doppler swinging, and a microwave wind radar.

These instruments are shown in Figure 1. At the same time, the UAS is attached with a radiosonde, so that nearly co-located measurements are made at the same time at the UAS and the radiosonde (right panel of Figure 1). The radiosonde in use is Vaisala RS41, with technical specifications meeting the upper-air measurement requirements of the World Meteorological Organization (WMO).

Two flight routes were adopted for the evaluation of the performance of meteorological measurements with the UAS. Firstly, the UAS hovered at around 25 m above ground level (AGL) near the wind mast, enabling direct comparison between the UAS wind measurements and the corresponding wind mast observations. In this process, the 1 s wind data of both instruments were processed to become 1 min mean winds for direct comparison. Secondly, the UAS was configured to fly vertically upwards from a height of 30 m to around 390 m AGL, increasing altitude in 30 m increments. At each level, a circular path is executed, as shown in the flight plan in Figure 2. The wind data collected with the UAS were compared with measurements from the radiosonde attached to the aircraft and ground-based remote-sensing equipment.

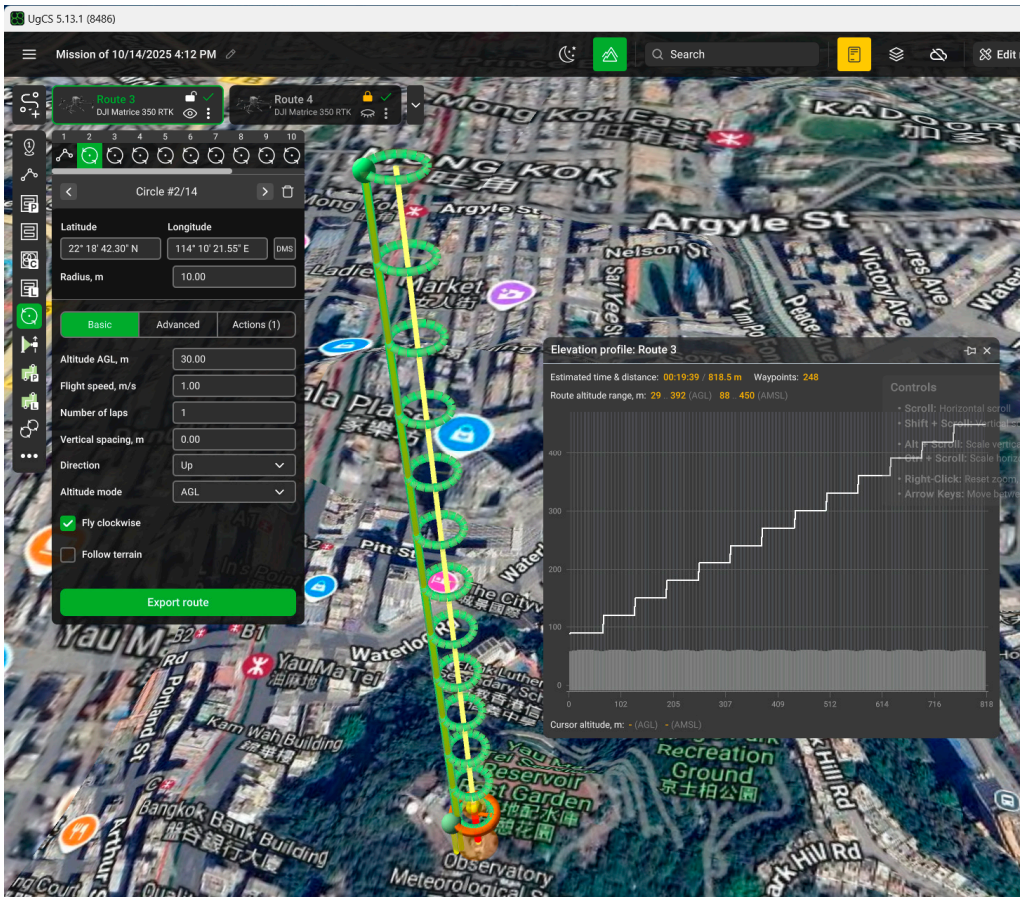
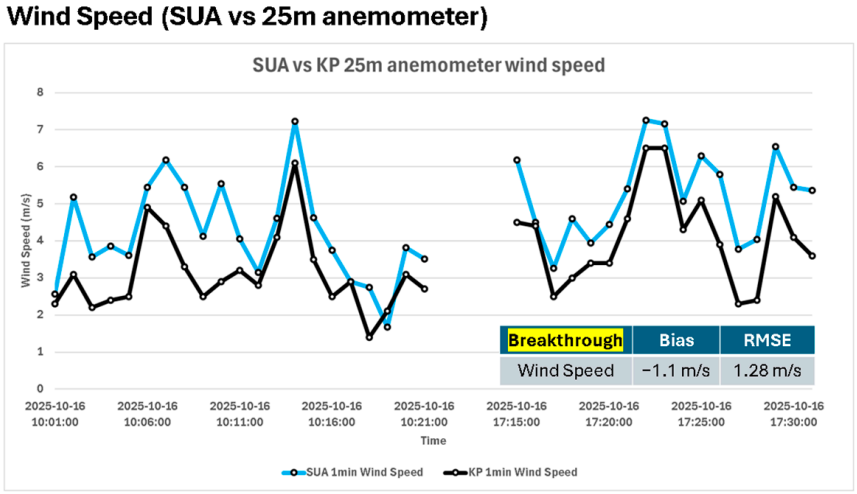


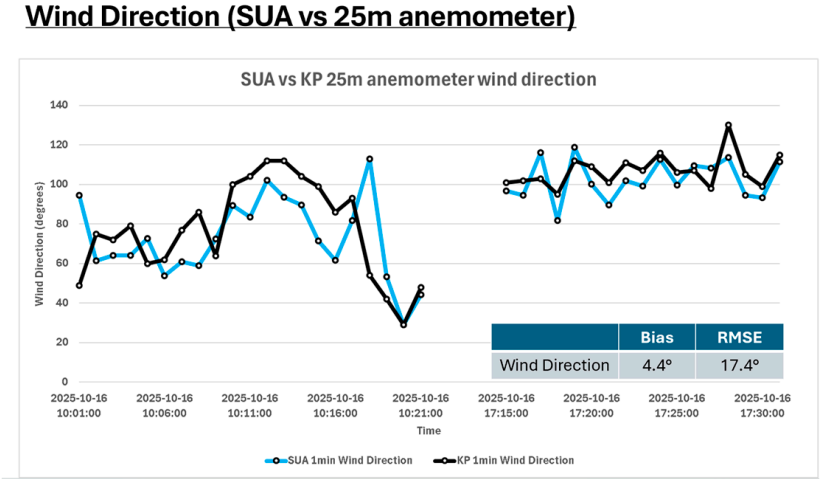
Figure 2. The vertical profiling flight route (line in green) at King's Park overlaid onto a map labeled in Chinese and English. The inset shows the vertical cross section (line in white) of the flight.

Figure 3a,b are the comparison results between the UAS and the wind mast data for the hovering flight, for wind speed and wind direction respectively. The meteorological measuring requirements of WMO (2025) [8] have been adopted. Two hovering flights were performed, one in the morning (local time) and another in the late afternoon. The results show that the root-mean-square-error (RMSE) of wind speed meets the "breakthrough" category of WMO, with a relatively small bias, as shown in Figure 3a. The wind directions measured by both instruments are generally consistent with each other as well, with an

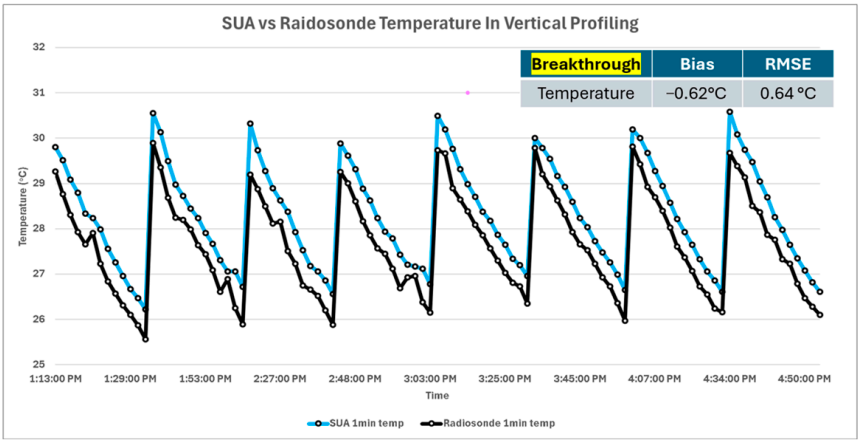
RMSE of about 20 degrees and a rather small bias. Figure 3c,d show the comparison results with radiosonde in the vertical profiling flight, for temperature and relative humidity (RH) respectively. Again, the RMSEs for both parameters meet the "breakthrough" level requirement of WMO, with an RMSE of around 0.6 degrees Celsius for temperature and around 2% for RH. The biases are generally small.



(**a**)

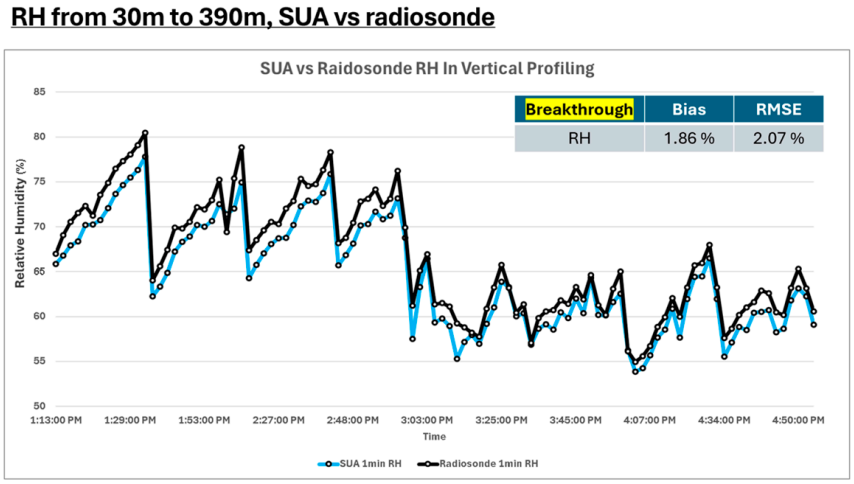


(**b**)



(**c**)

Figure 3. *Cont.*



(**d**)

Figure 3. The comparison between UAS and wind mast (**a**,**b**) radiosonde (**c**,**d**) during hovering flight at King's Park.

Figure 4a shows the comparison for wind speed between UAS and the remote-sensing equipment, including the LIDAR (the one on the left-hand side in the inset of Figure 1) and microwave radar. The RMSEs are generally less than 2 m/s, with relatively small biases. In particular, the microwave radar has been found to slightly over-estimate the wind speed in comparison with both UAS and LIDAR measurements. This feature has been found in the field test of this microwave radar for some months in Hong Kong (results to be reported separately).

Furthermore, the UAS 1 s wind data have been used to calculate TKE within a period of 1 min from 1 s wind components, computed as TKE = 0.5 ($\sigma u^2 + \sigma v^2 + \sigma w^2$) [9–11]. The 1 min TKE at different heights as measured by the UAS are shown in Figure 4b. In general, it is found to be decreasing with height, consistent with the expectation of higher turbulence nearer the ground. To explore the vertical wind profile further, the 1 min mean wind speed data have been plotted against height and fitted with a logarithm (log) law [9,12], as shown in Figure 4c. The fitting with the log law turns out to have a rather good correlation coefficient squared (around 0.345) and a small RMSE (around 1.15 m/s). The friction velocity and roughness length calculated from the fitted equation are shown in Figure 4c. Only a few data points could be collected for each vertical profiling. To gather a larger dataset, data across multiple profiles are combined, leading to a larger dispersion of data points for each AGL height. However, the fitting appears to be reasonable for the boundary layer within the urban area [13].

2.2. UAS Measurement Methodology and Results at Peng Chau (Sandbox Project Location)

Peng Chau is a hilly C-shaped island with a bay facing the east-northeast. There is no road connection to this island from other areas of Hong Kong and thus transportation to this island is mainly made by marine vessel to the piers of this island. A sandbox project on this island will use a UAS to transport materials from a beach in the northwest, across a bay, to a site on a hilltop at the southeastern side. The flight route is shown in Figure 5a. Two UAS missions were conducted to collect meteorological data to better understand the atmospheric environment over the sandbox route. For the first mission, the UAS performed a round trip flight between the beach and the hilltop, as shown in Figure 5b for the flight route in a three-dimensional picture and the vertical cross section in the inset. In the second mission, the UAS carried out vertical profiling at designated locations over the bay and hill of Peng Chau to obtain information about the surface roughness characteristics of the

region. The vertical profiling flight pattern was similar to that at King's Park but was conducted at five specific locations.

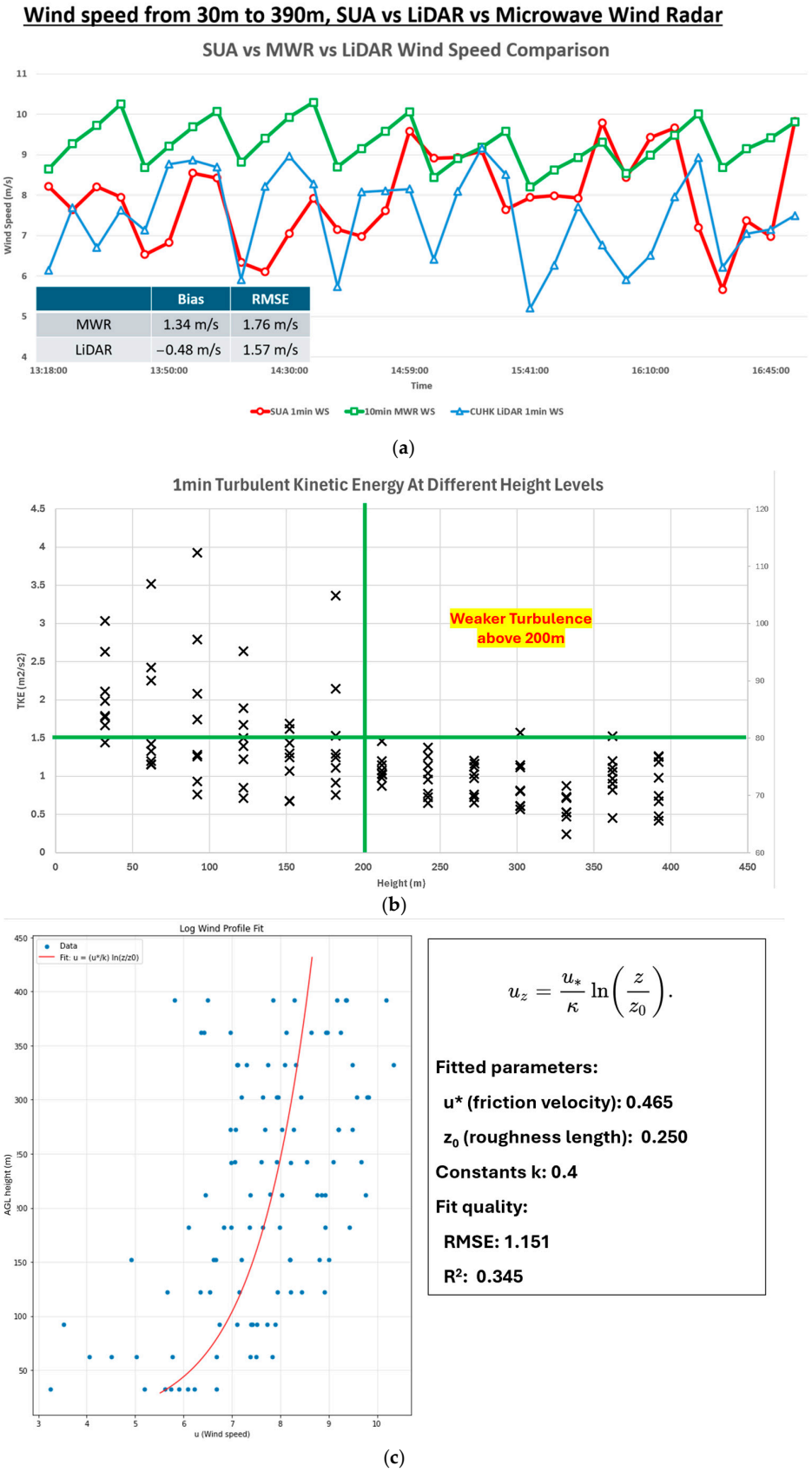
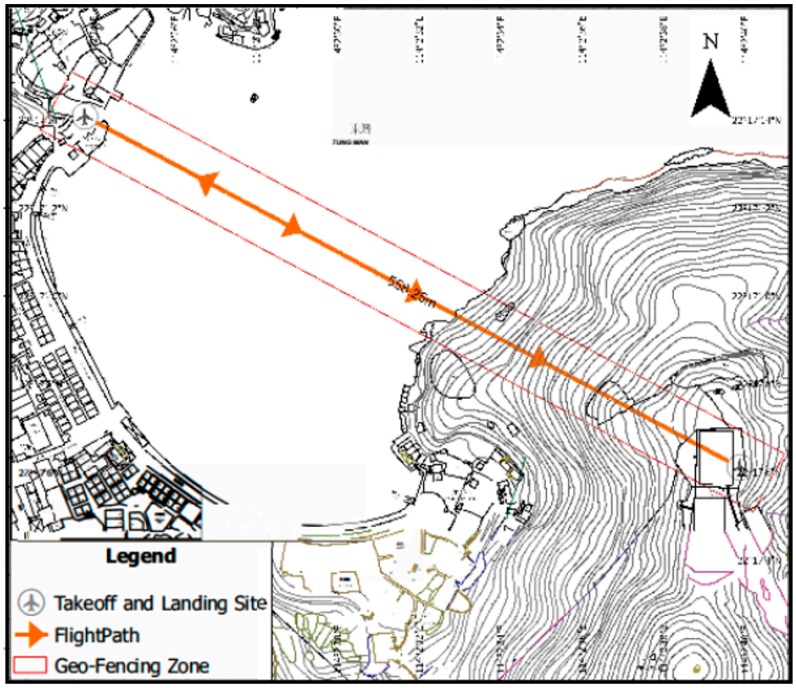
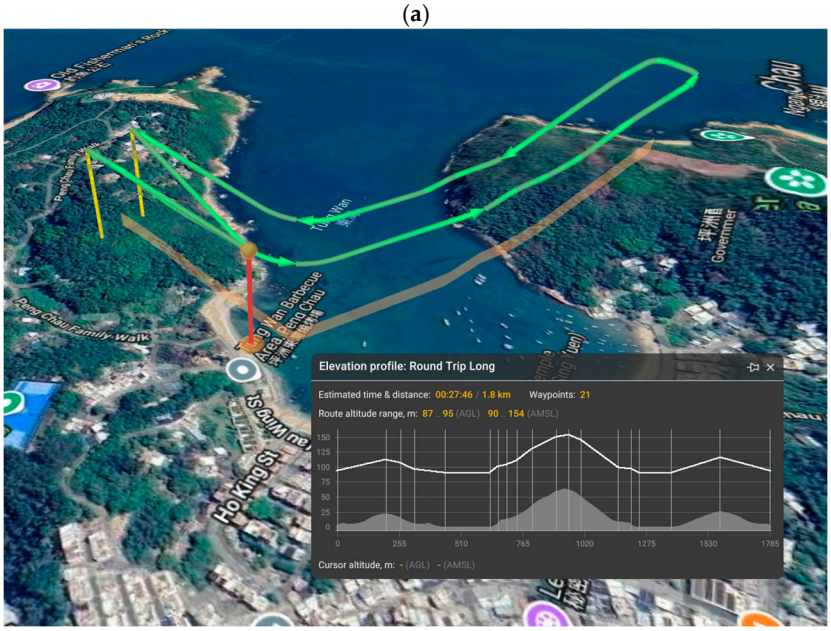


Figure 4. Comparison of upper wind speed (**a**), vertical TKE profile (**b**) and vertical wind profile (**c**).

The first mission was conducted for most of the afternoon of 23 October 2025 under prevailing northerly winds in Hong Kong. Samples of 1 min TKE and 1 min mean wind speed and direction data are shown in the left and the right-hand side panels of Figure 6a respectively. Wind measurements from the UAS show that prevailing northerlies were affecting the region, with mean wind speed varying between about 8 to 10 m/s, and no particular pattern is observed in the mean wind speed. For TKE, it is found to be higher at the uphill and downhill locations. The time series of 1 min mean wind speed, 1 min TKE and the altitude of the aircraft is shown in Figure 6b. No special pattern shows up in the time series of wind speed, such as any correlation with the altitude of the aircraft, but relatively higher TKE of over 3 m^2/s^2 was observed during the downhill flight.



(**a**)



(**b**)

Figure 5. The round trip flight route (in green line) at Peng Chau overlaid on a map labeled in Chinese and English. The direction of the flight is shown through the direction of the arrows. The sandbox route at Peng Chau (**a**) and the round trip flight (**b**).

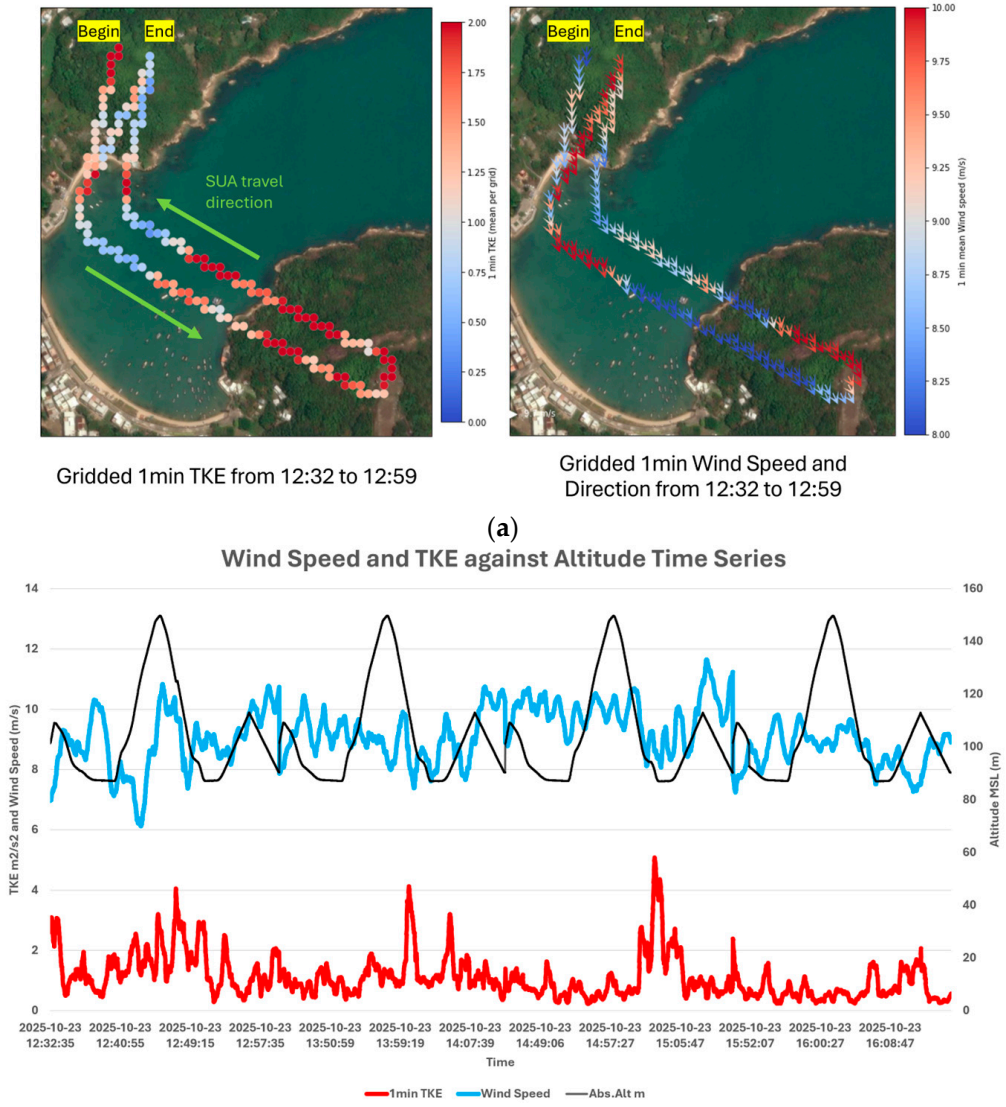
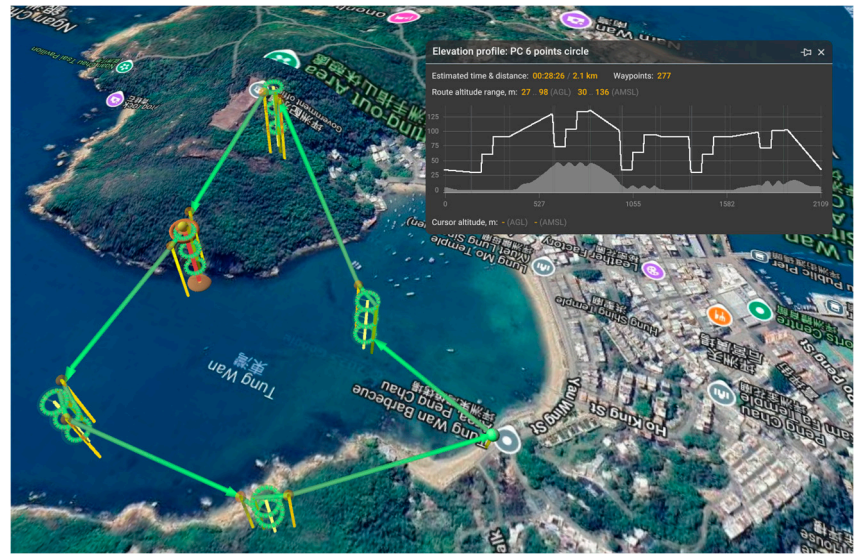
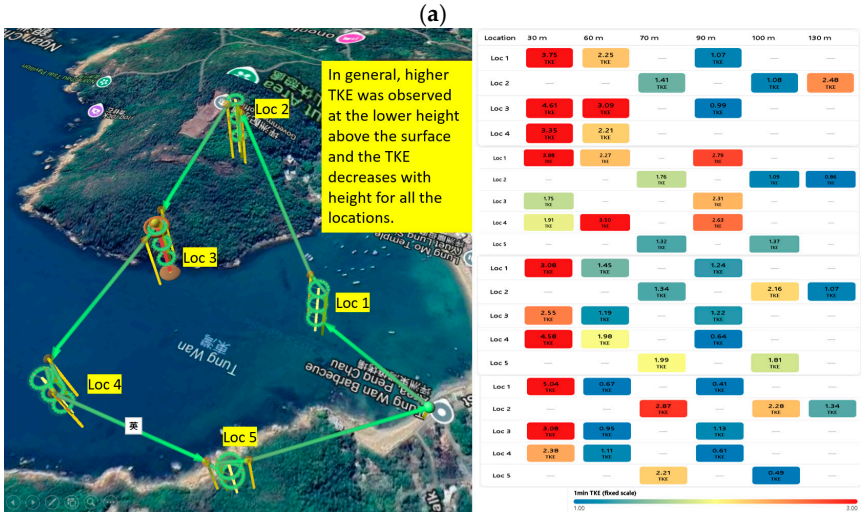


Figure 6. (**a**) shows a sample of TKE data collected by round trip flight (**left-hand side**) and the wind speed data collected (**right-hand side**). (**b**) gives the time series of wind speed, TKE and altitude of the UAS.

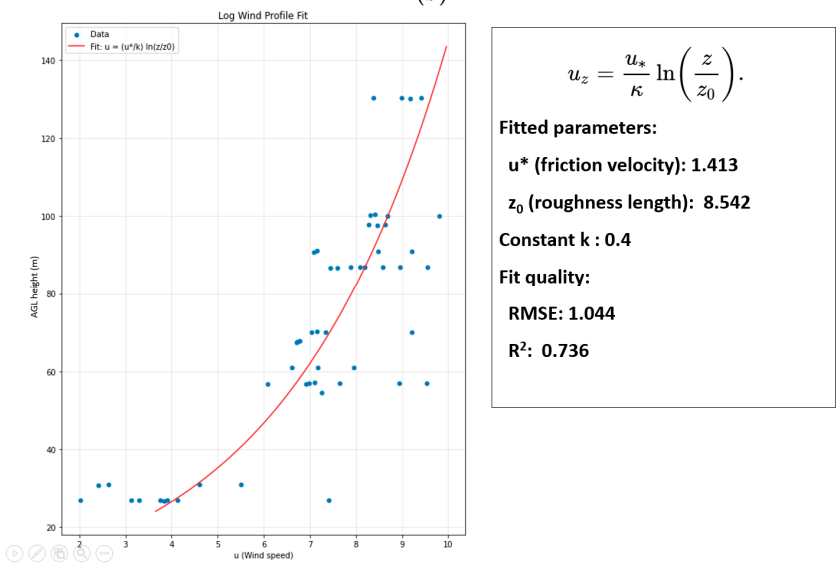
For the second mission, similar to the vertical profiling flight at King's Park, TKE is found to decrease generally with altitude at all five locations (Figure 7b). No particular pattern shows up in the spatial variability of the TKE. The vertical profile of 1 min mean wind is again fitted with the log law as in the case of King's Park vertical profiling. Since there is only a limited number of data points for the vertical profiling at each location, profiles at different locations were combined to yield a larger dataset, such that the fitting could be better represented. The data were well fitted (Figure 7c) with a rather high correlation coefficient squared (around 0.736) and a generally small RMSE (around 1 m/s). The friction velocity is reasonable. On the other hand, the roughness length is particularly high, as compared with the results in [13]. This may be related to the complex land–sea contrast and hilly terrain in the region under investigation [14,15].



(**a**)



(**b**)

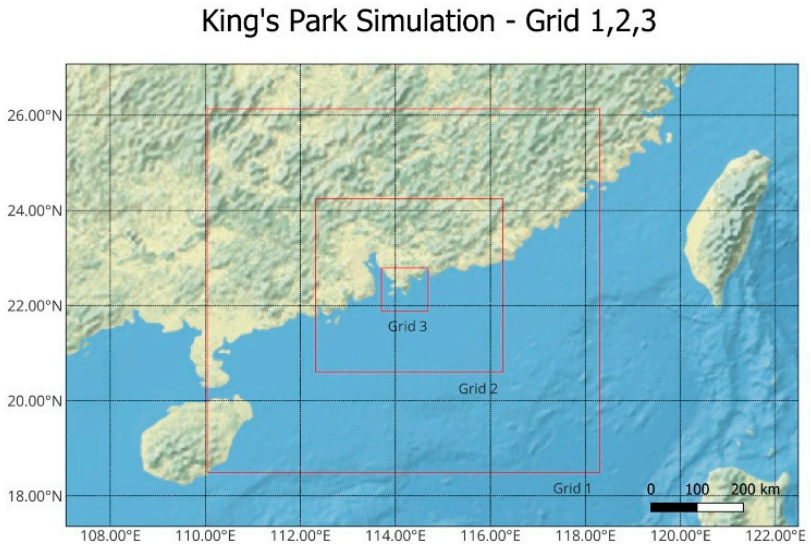


(**c**)

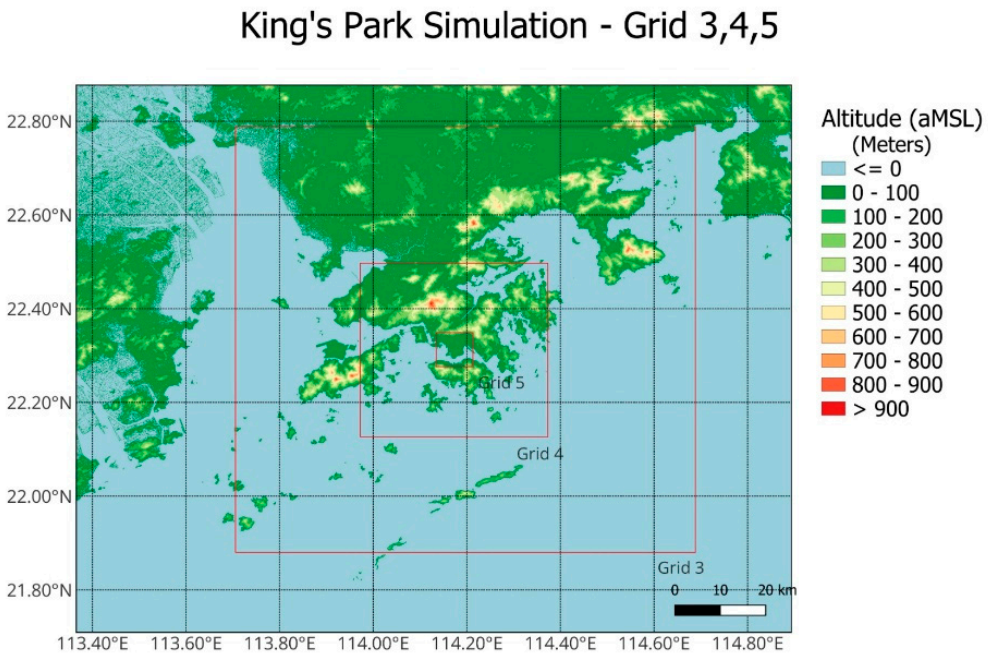
Figure 7. (**a**) shows the route of the vertical profiling flight (in green line) overlaid on a map labeled in Chinese and English; (**b**) shows the TKE data at each location and at different altitudes overlaid on a map labeled in Chinese and English; (**c**) gives the vertical profile and log law fitting (in red line) for wind speed.

3. Setup of Numerical Weather Prediction Modelling

In order to further study the data collected by the UAS, a high-resolution NWP simulation has been performed, following the method adopted for studying terrain-induced low-level windshear at the Hong Kong International Airport (HKIA). The Regional Atmospheric Modelling System (RAMS) version 6.3 is used in this study [16,17]. It is nested with the re-analysis data of the European Centre for Medium Range Weather Forecast (ECMWF) with a spatial resolution of 25 km. Five nests have been performed, with spatial resolution of 25 km, 5 km, 1 km, 200 m and 40 m. Two simulations have been conducted, one centred at King's Park and another at Peng Chau. The five model domains of the former simulation could be found in Figure 8a,b. For the simulation at Peng Chau, the first two grids are similar to those in Figure 8a, and the last three grids are shown in Figure 8c.

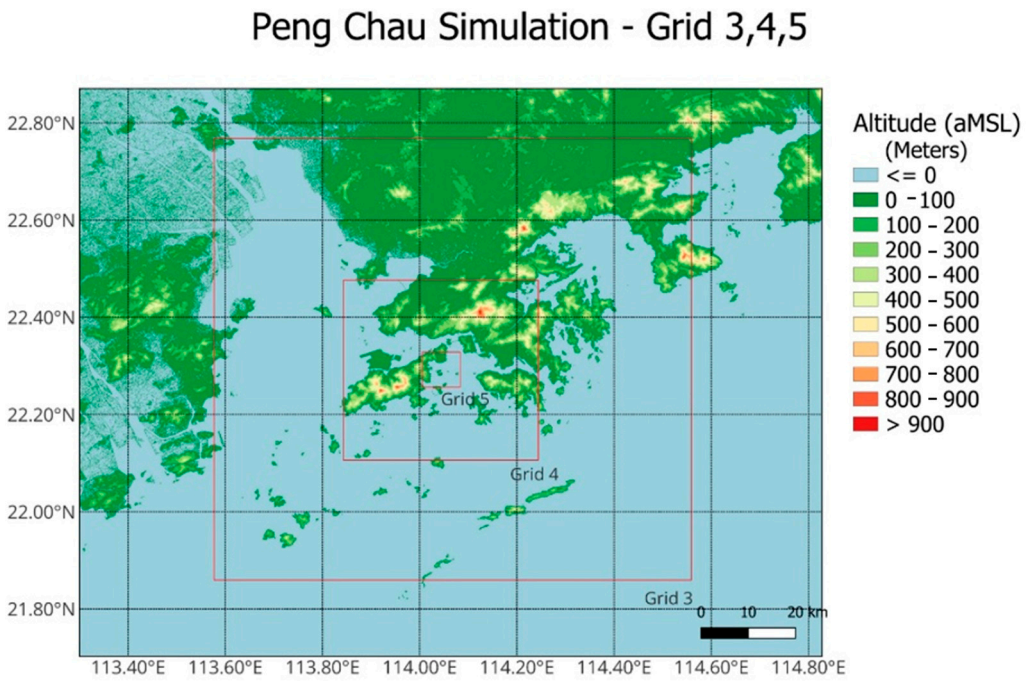


(**a**)



(**b**)

Figure 8. *Cont.*



(**c**)

Figure 8. The model domains for King's Park simulation (**a**,**b**). (**c**) shows the domains (in red lines) of grids 3 to 5 for the simulation at Peng Chau.

The turbulence parameterization scheme is important for the successful reproduction of the wind features as affected by the local terrain. Zhang et al. recently highlighted how LES turbulence closures in WRF over hills/topography influence separated flows and near-surface winds [18]. Li et al. also mentioned that urban parameterization choices in mesoscale models are another key uncertainty source [19]. For the first two grids, the Smagorinsky scheme [20] has been adopted. For the last three grids, the Deardorff scheme [21] is used to perform simulations at large eddy simulation (LES) mode. The choice of these schemes has been well established in the studies of low-level wind features at HKIA [22], such as comparison between the model-simulated winds and the actual observations from the ground-based anemometers and remote-sensing LIDARs.

4. Comparison of UAS Measurements with NWP Results

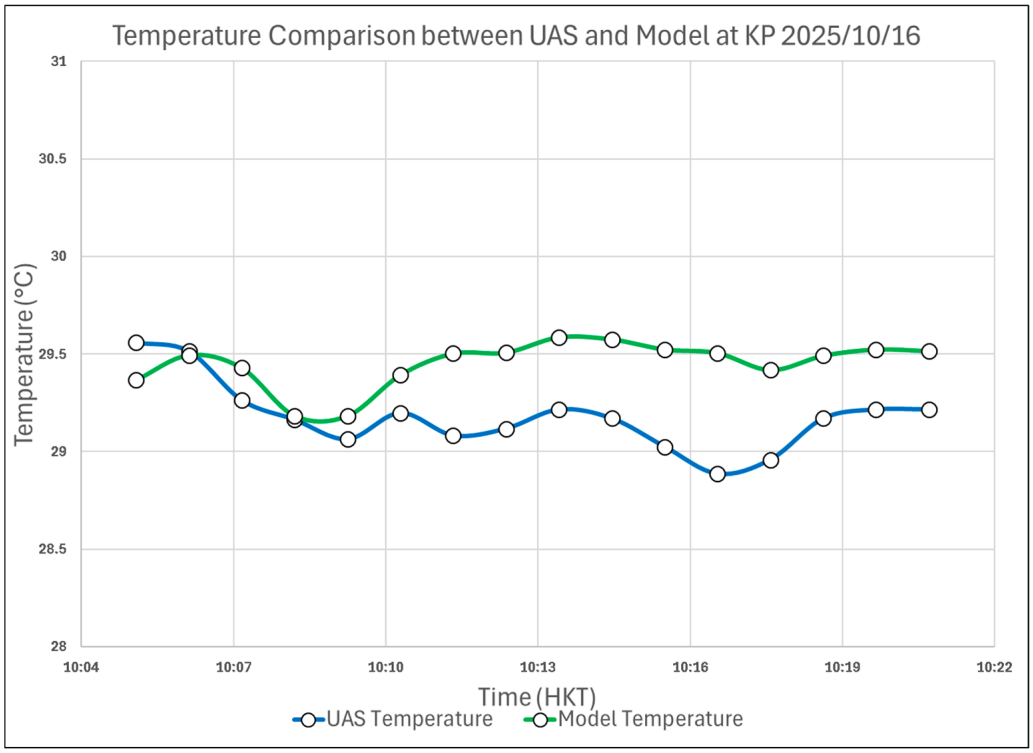
This section presents a systematic comparison between UAS measurements and high-resolution NWP simulation results. Six meteorological parameters are evaluated: temperature, relative humidity, pressure, turbulent kinetic energy (TKE), wind speed, and wind direction. These parameters were selected based on their operational relevance for LAE flight safety and planning. In particular, TKE serves as a key indicator of atmospheric turbulence that directly impacts flight stability, and we aim to evaluate whether NWP models can accurately forecast this parameter. Comparisons are conducted for two flight types (hovering flight and vertical profiling flight) at King's Park, and two flight types (round trip flight and vertical profiling flight) at Peng Chau. The morning of 16 October 2025 was selected for the King's Park hovering flight comparison as it represented a period of relatively stable atmospheric conditions with prevailing northerly winds. Clear weather conditions during this period minimized confounding factors from precipitation or extreme weather events.

Figure 9 shows the comparison results for the hovering flight at King's Park in the morning of 16 October 2025. Six elements have been involved in the comparison, namely, temperature, RH, pressure, TKE, wind speed and wind direction. The evaluation statistics

are summarized in Table 2, including bias, RMSE and correlation coefficient. In general, the biases are rather small for temperature, pressure, wind speed and wind direction. The RMSEs are generally on the low side, apart from the wind direction, and TKE, which is of a similar order of magnitude as the absolute value of the TKE itself. The higher RMSE of the wind direction could be expected as King's Park is surrounded by buildings and trees in the vicinity, and an RMSE of around 40 degrees should be considered to be satisfactory in view of the complexity of the environment. Similar argument may apply for the RMSE of TKE. Another simulation using a computational fluid dynamics (CFD) model coupled with RAMS output is being conducted, and hopefully the RMSE could be reduced with a more realistic representation of the buildings. The correlation coefficients do not appear to be satisfactory, but this is understandable given the relatively short period of flight considered.

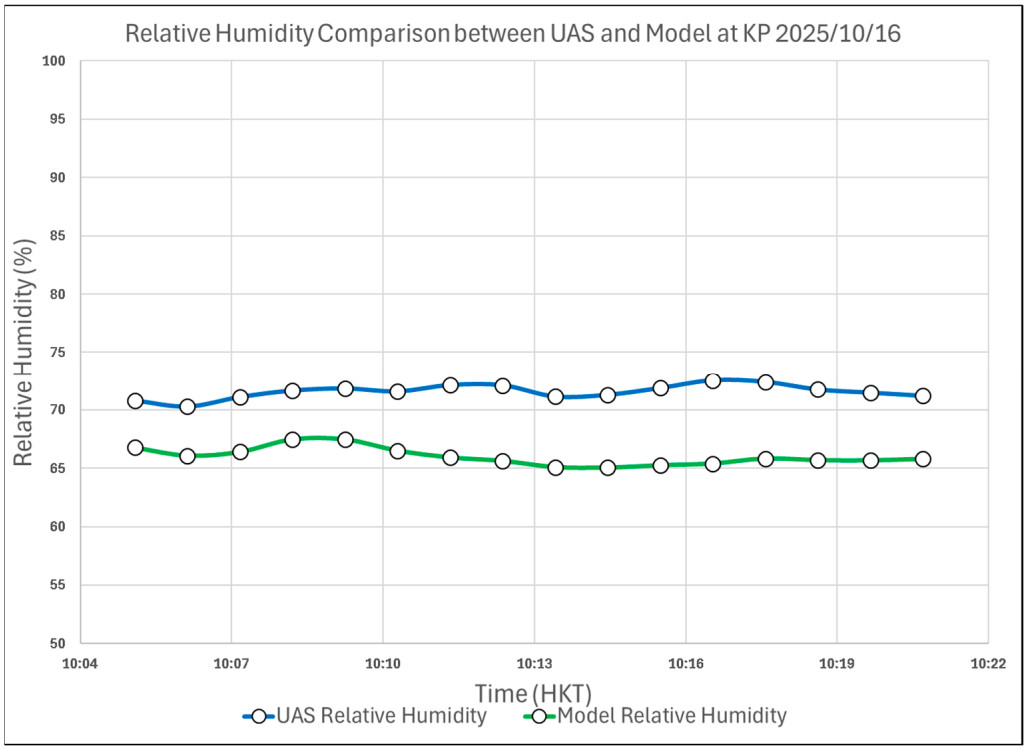
Figure 10 shows the comparison results for the vertical profiling flight at King's Park, and the evaluation statistics are given in Table 3. In general, the correlation is much better compared to the hovering flight, particularly for temperature, pressure, wind direction and TKE, because the range of variation in these parameters is higher in a vertical profiling flight compared with a hovering flight at about the same height. However, a rather large bias still shows up in RH and wind direction. Again, the latter is related to the complexity of the environment, and the former may be related to the difficulty of NWP in general in accurately simulating RH. The RMSE result shows that the simulation for TKE remains challenging in a complicated urban environment.

A sample simulation result of TKE and horizontal wind field at a height of 129 m above sea level is shown in Figure 11a,b respectively. King's Park is located on top of a hill of around 66 m above sea level and higher TKE is found downstream of the hill in the prevailing east to southeasterly flow.

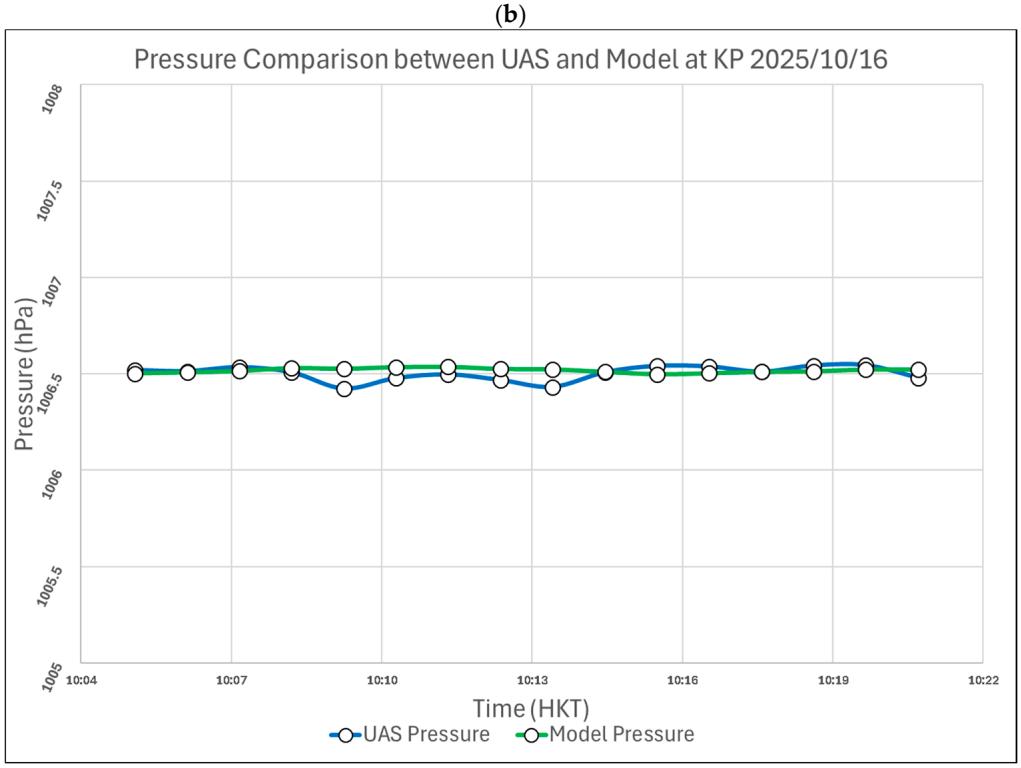


(**a**)

Figure 9. *Cont.*

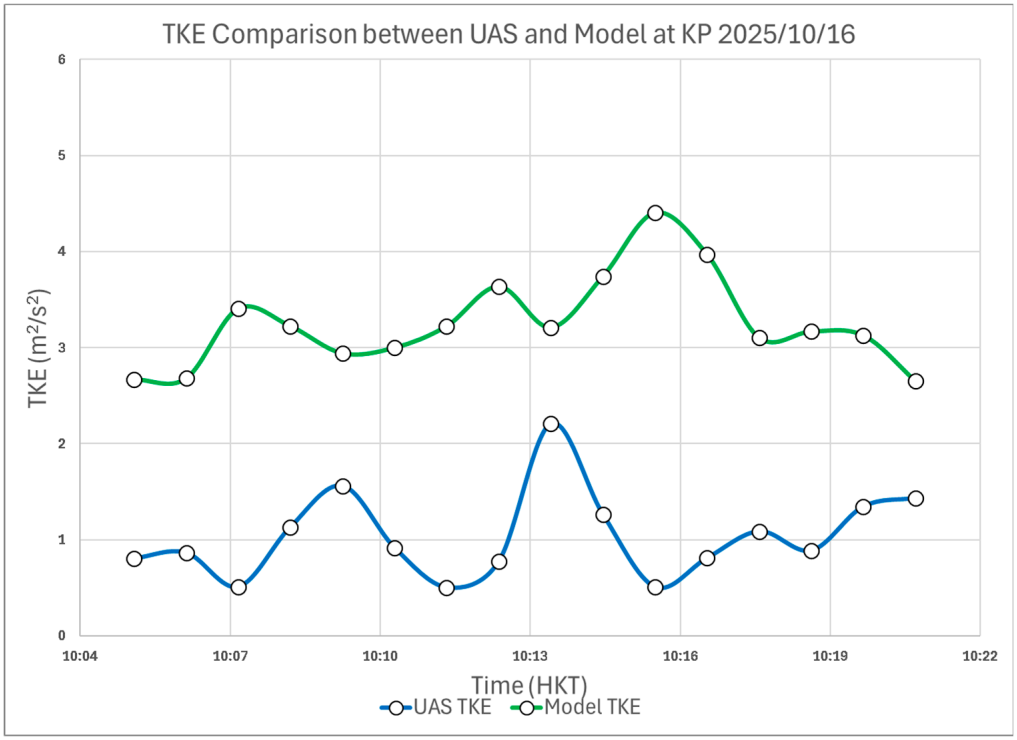


(**b**)

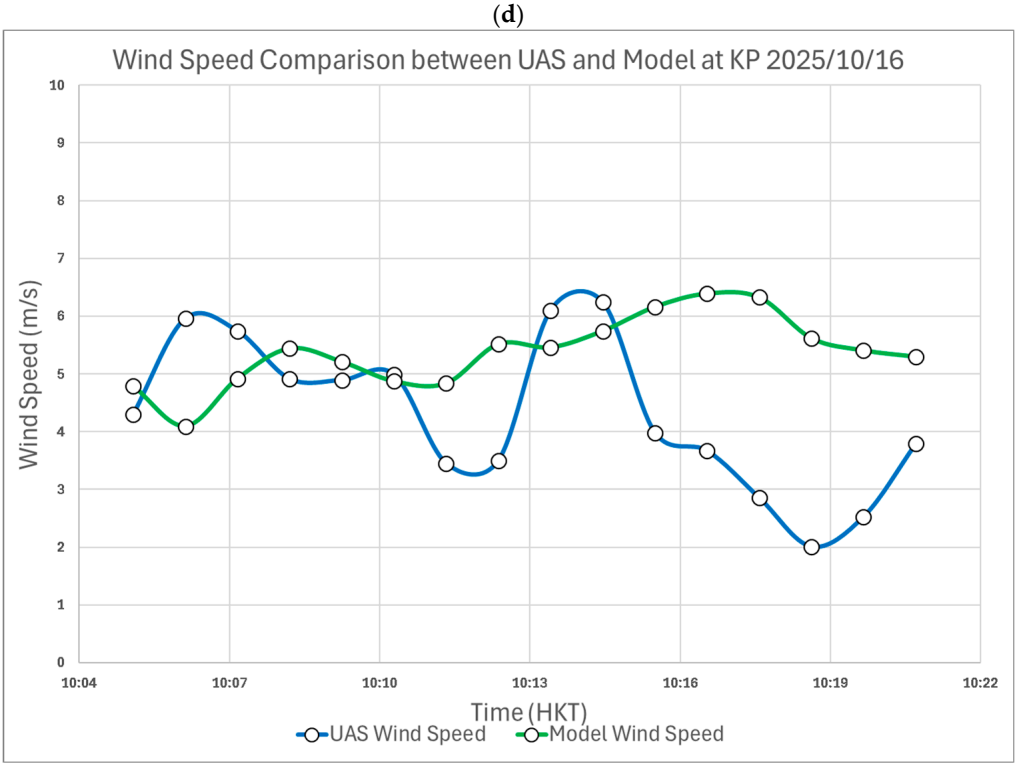


(**c**)

Figure 9. *Cont.*

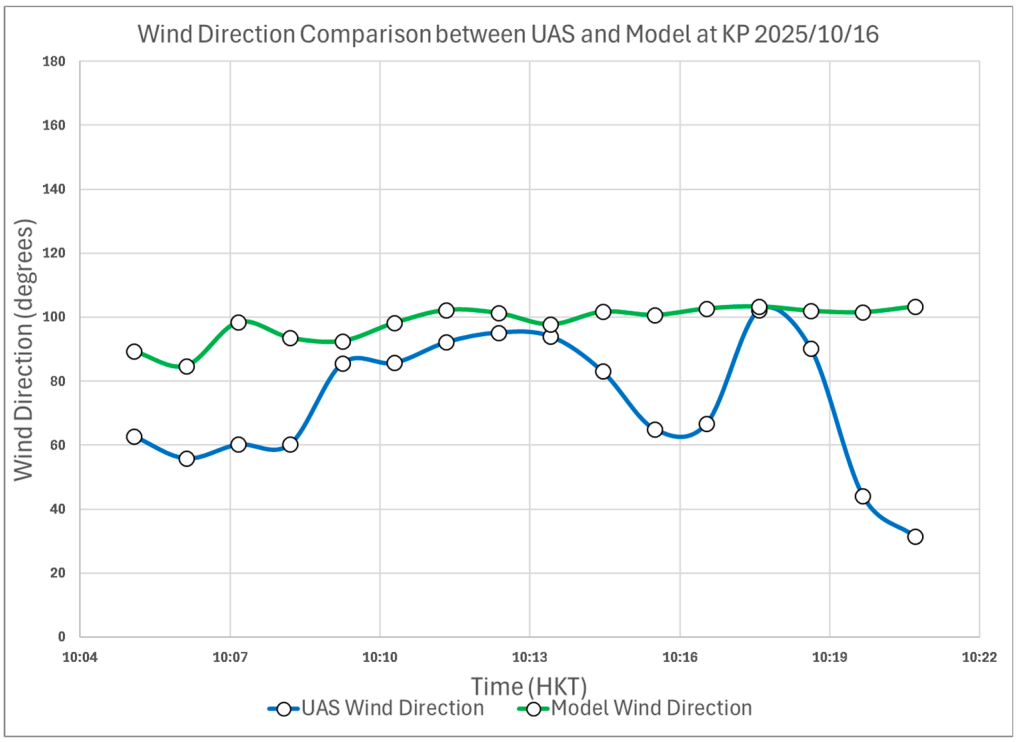


(**d**)



(**e**)

Figure 9. *Cont.*



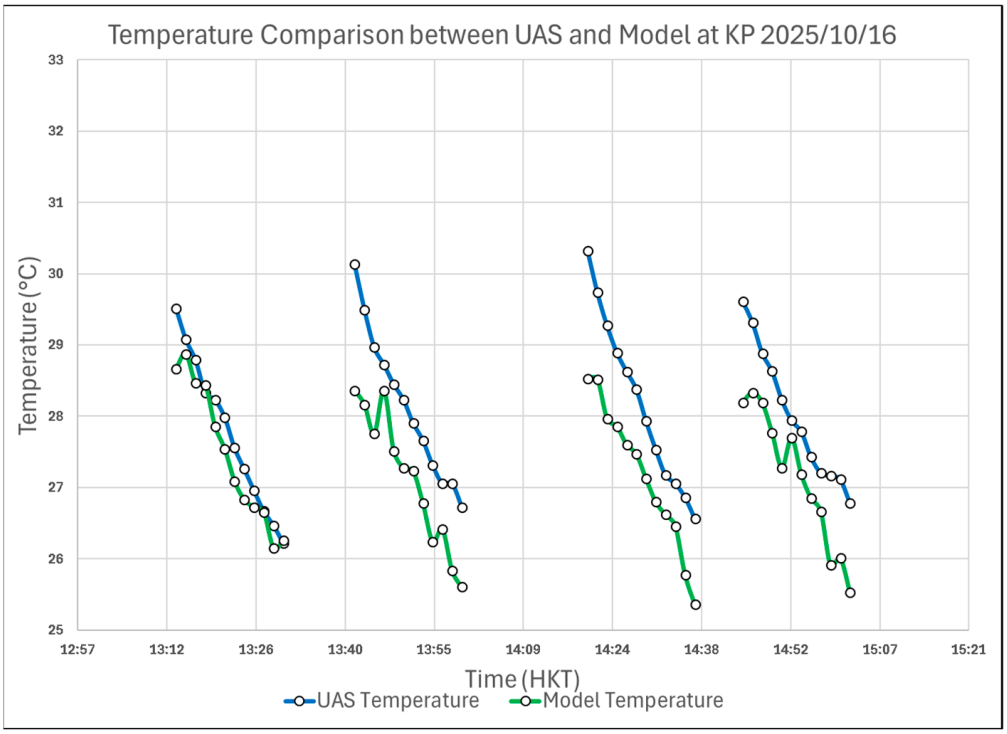
(**f**)

Figure 9. The time series of observed and simulated temperature (**a**), RH (**b**), pressure (**c**), TKE (**d**), wind speed (**e**) and wind direction (**f**) for the hovering flight at King's Park.

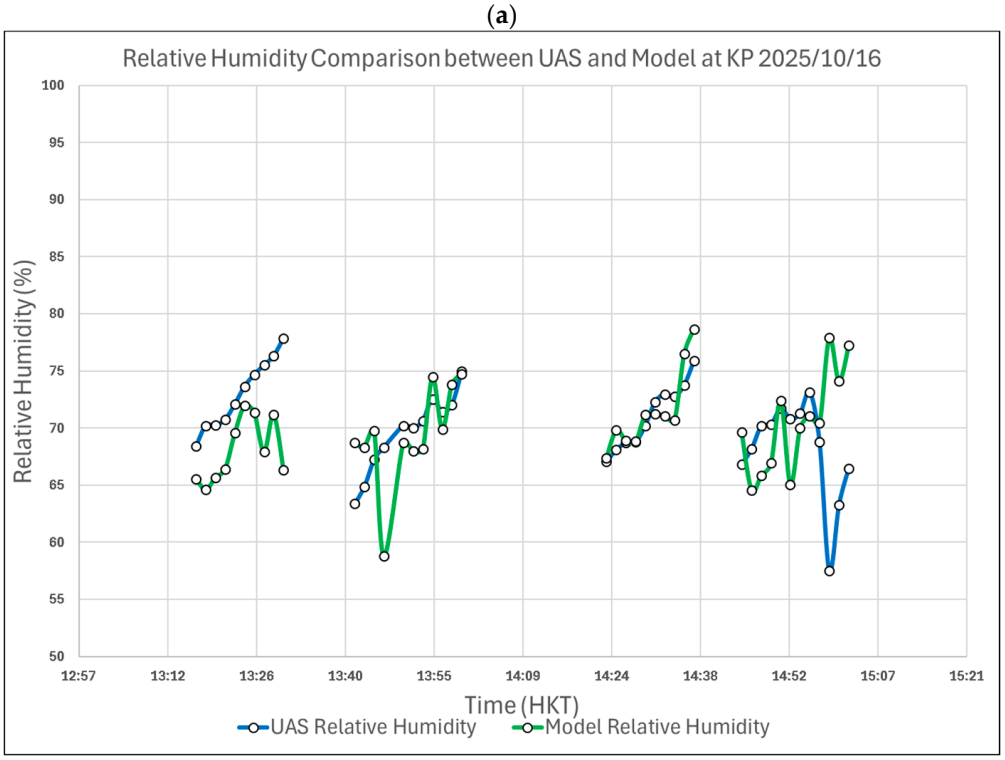
Table 2. Statistics for the hovering flight at King's Park.

	Temperature (°C)	Relative Humidity (%)	Pressure (hPa)	TKE (m^2/s^2)	Wind Speed (m/s)	Wind Direction (Degrees)
RMSE	0.34	5.66	0.046	2.34	1.93	31.54
Bias	−0.27	5.57	−0.0015	−2.22	−1.07	−24.85
Correlation	−0.017	−0.13	−0.57	−0.32	−0.40	0.20

Figure 12 shows the comparison results for the round trip flight at Peng Chau and the evaluation statistics are given in Table 4. Correlations are reasonable for temperature, RH and pressure, though the bias and RMSE for RH are generally high. On the other hand, the simulation results tend to give horizontal winds with a more easterly component compared with the actual observations; thus, the evaluation statistics are not so satisfactory for wind direction. Accurate simulation of TKE is also challenging. While the simulated TKEs could reach similar maximum values as those observed from UAS in the various round trip flights (Figure 12d), time shifts between the observed and the simulated TKEs led to less than satisfactory correlation result. Similar observation is found for wind speed (Figure 12e), with much larger fluctuations of the simulated wind speed compared to the actual observations.

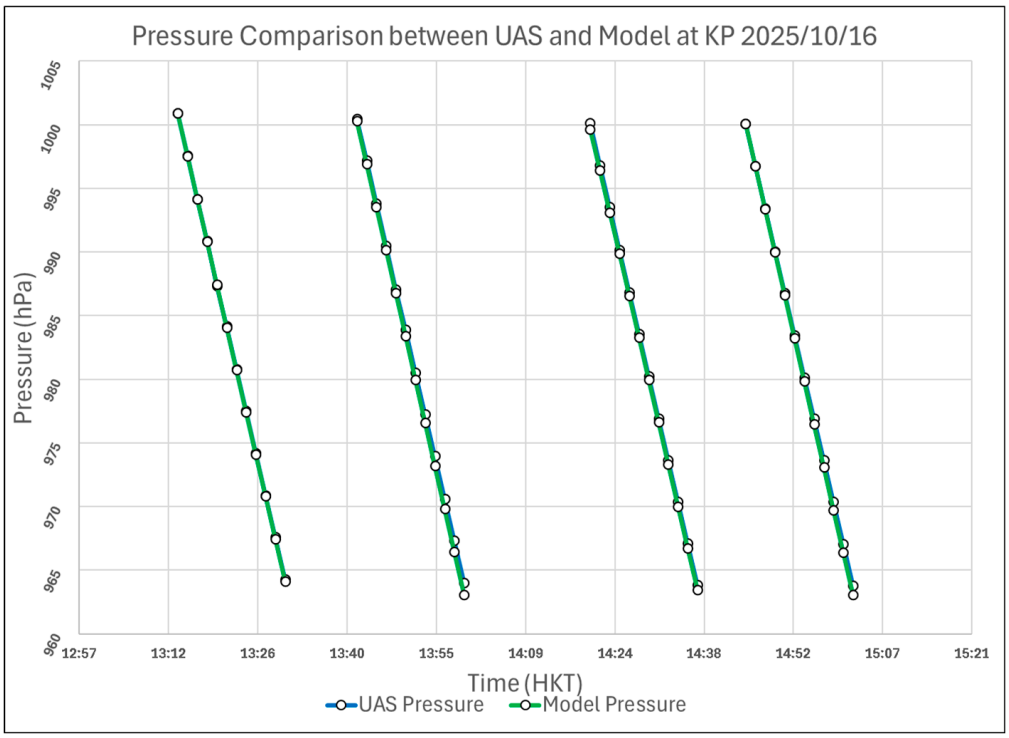


(**a**)

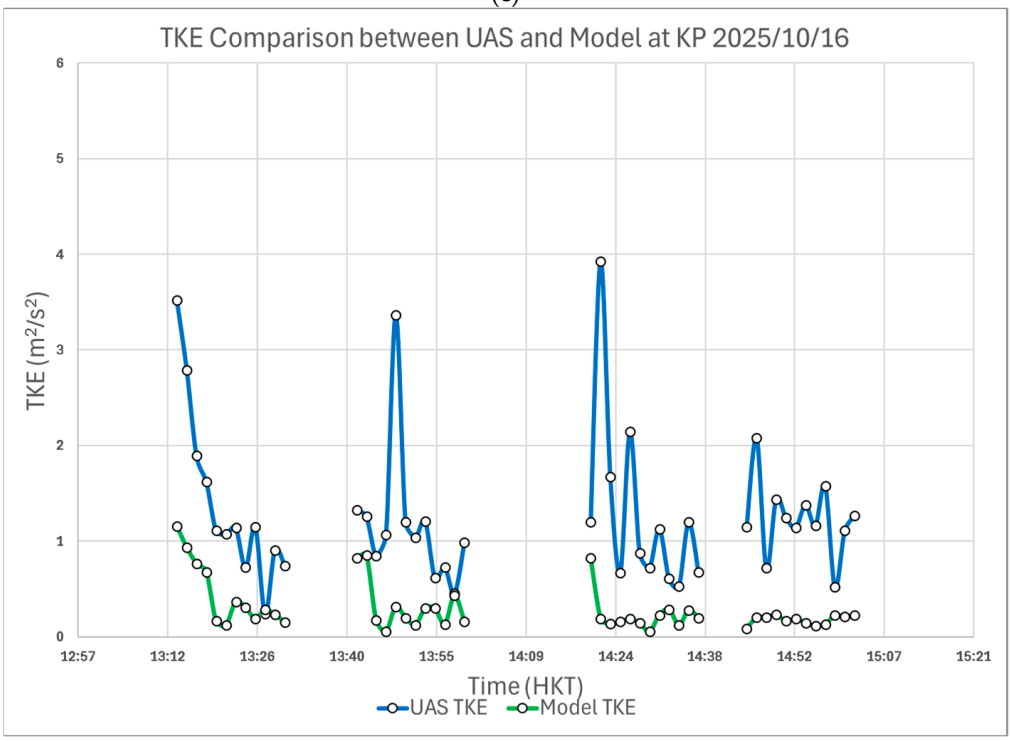


(**b**)

Figure 10. *Cont.*

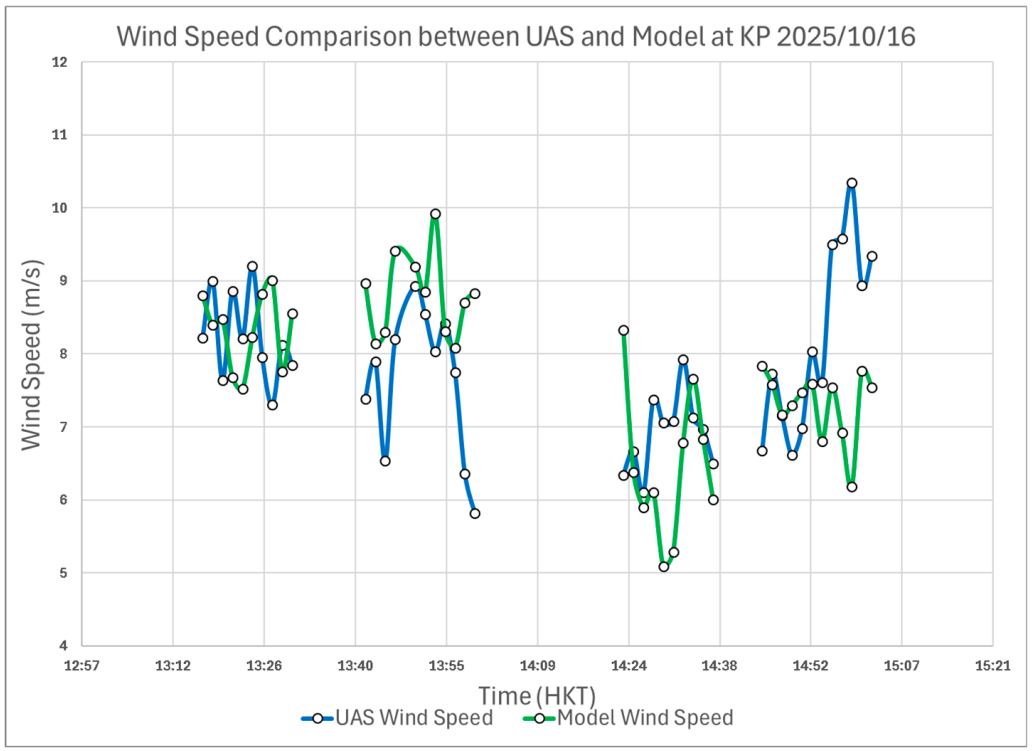


(**c**)

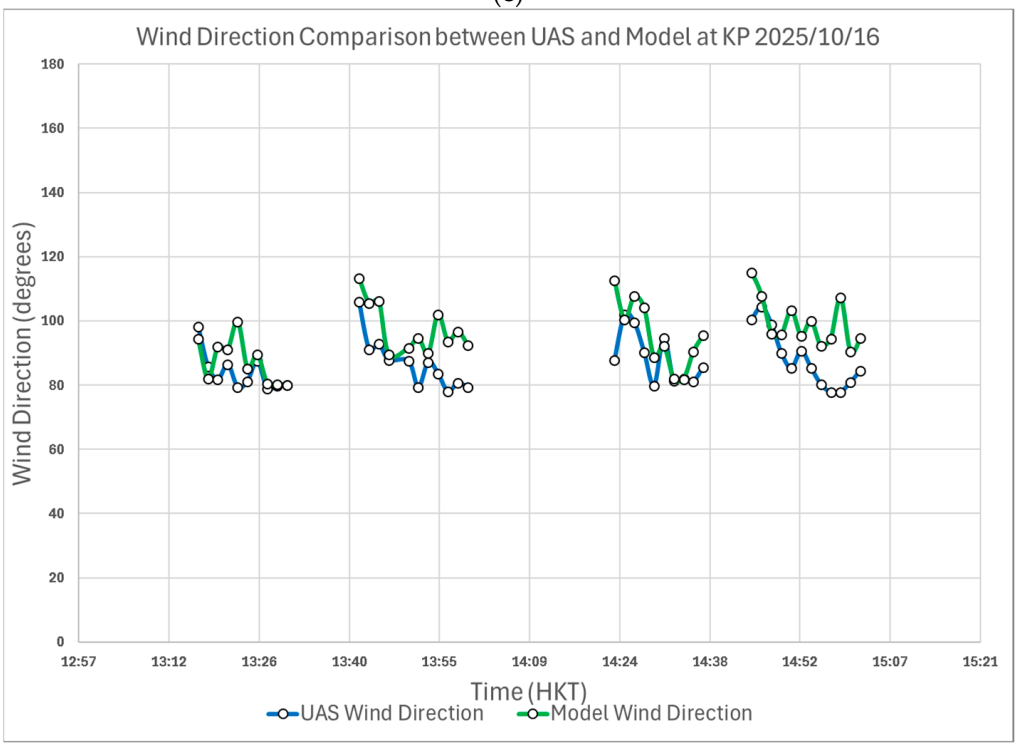


(**d**)

Figure 10. *Cont.*



(**e**)

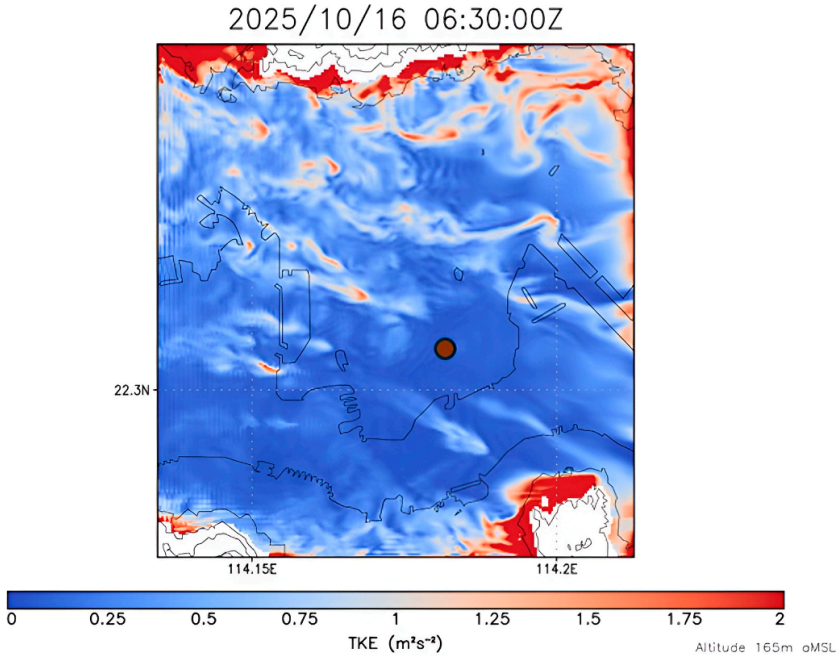


(**f**)

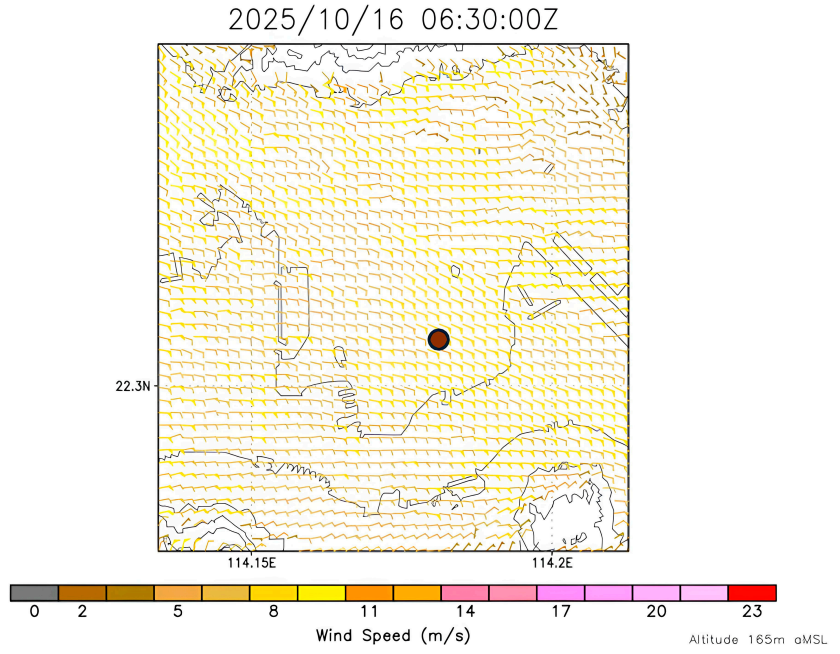
Figure 10. The time series of observed and simulated temperature (**a**), RH (**b**), pressure (**c**), TKE (**d**), wind speed (**e**) and wind direction (**f**) for the vertical profiling flight at King's Park.

Table 3. Evaluation statistics for the vertical profiling flight at King's Park.

	Temperature (°C)	Relative Humidity (%)	Pressure (hPa)	TKE (m^2/s^2)	Wind Speed (m/s)	Wind Direction (Degrees)
RMSE	0.88	5.38	0.42	0.93	1.40	11.59
Bias	0.78	0.49	−0.19	0.83	0.04	−8.50
Correlation	0.90	0.03	1.00	0.422	0.14	0.57

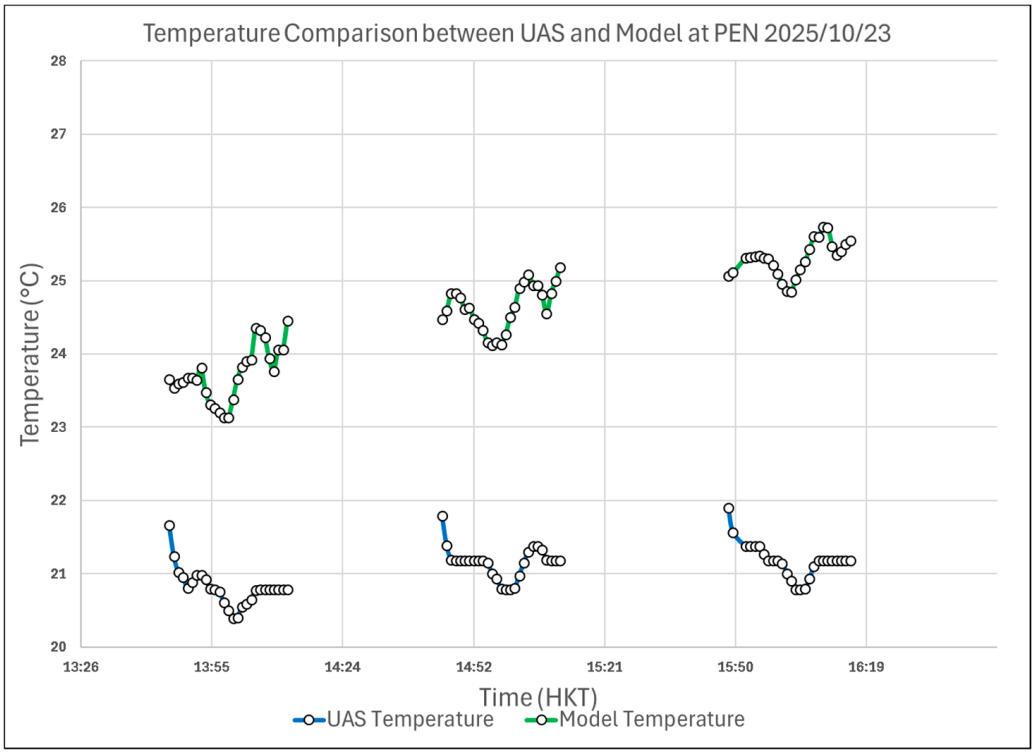


(**a**)

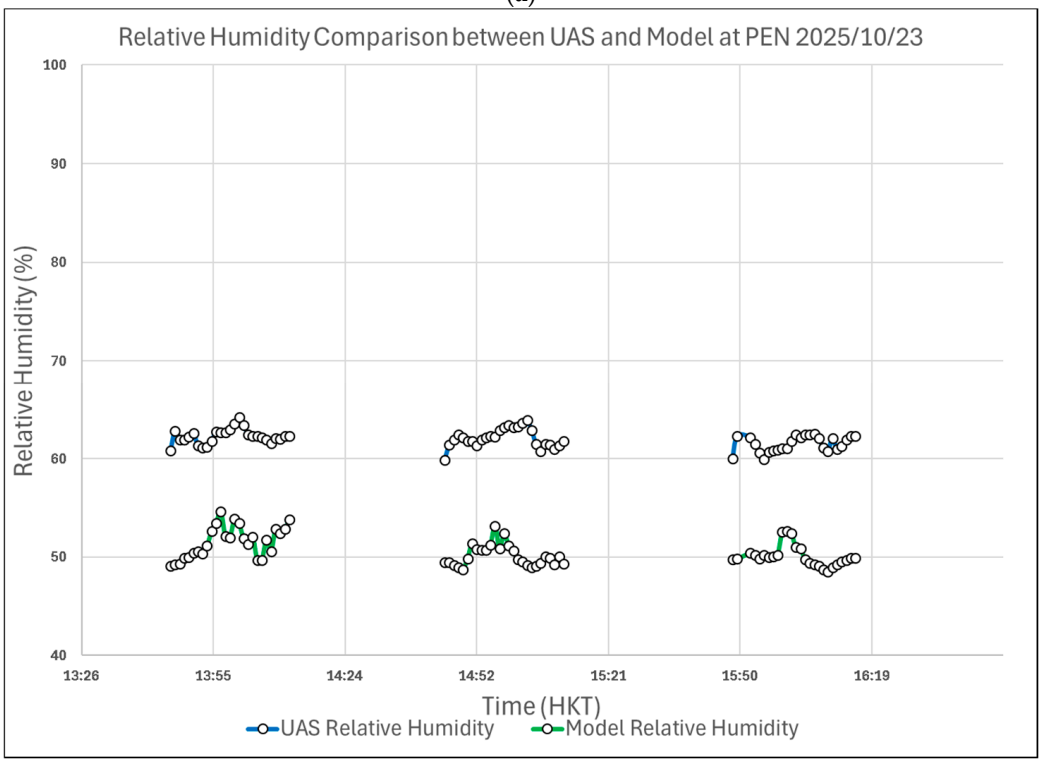


(**b**)

Figure 11. The simulated TKE (**a**) and horizontal wind (**b**) at a height of 129 m above sea level. The location of King's Park is given by a brown dot.

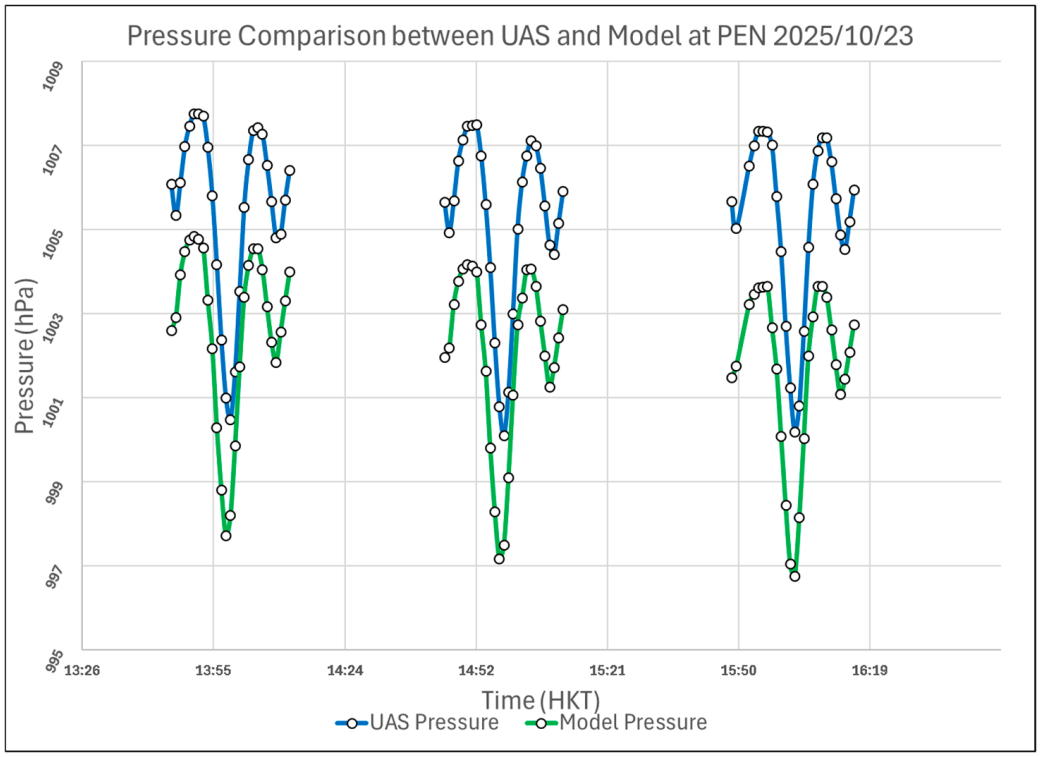


(**a**)

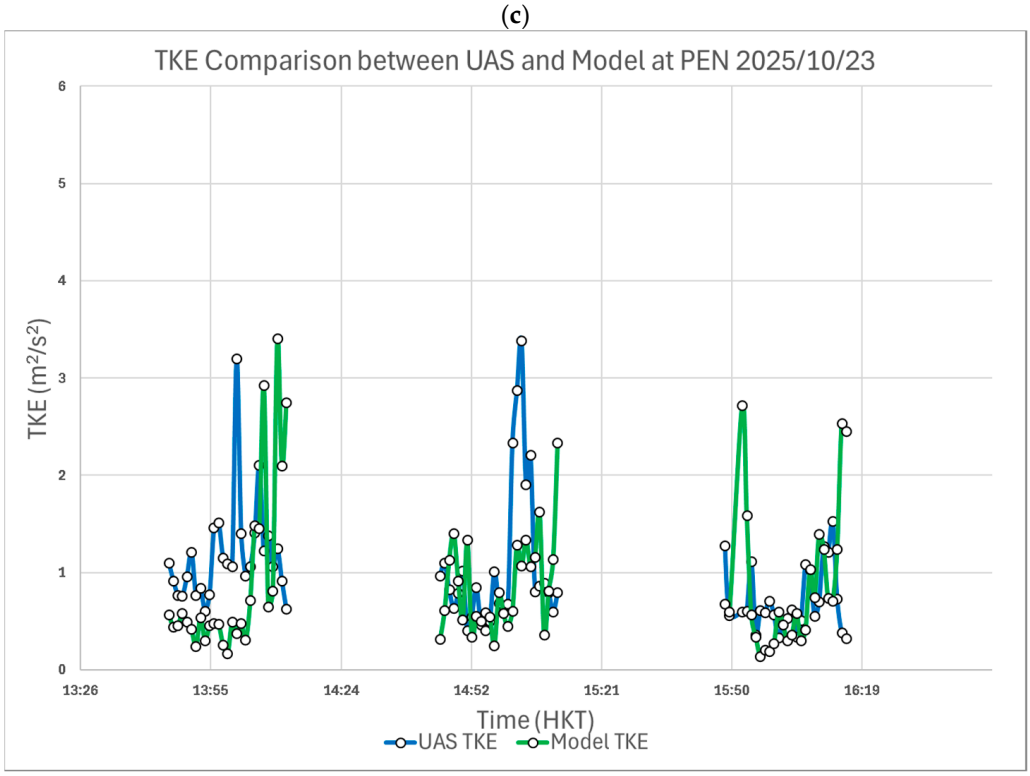


(**b**)

Figure 12. *Cont.*

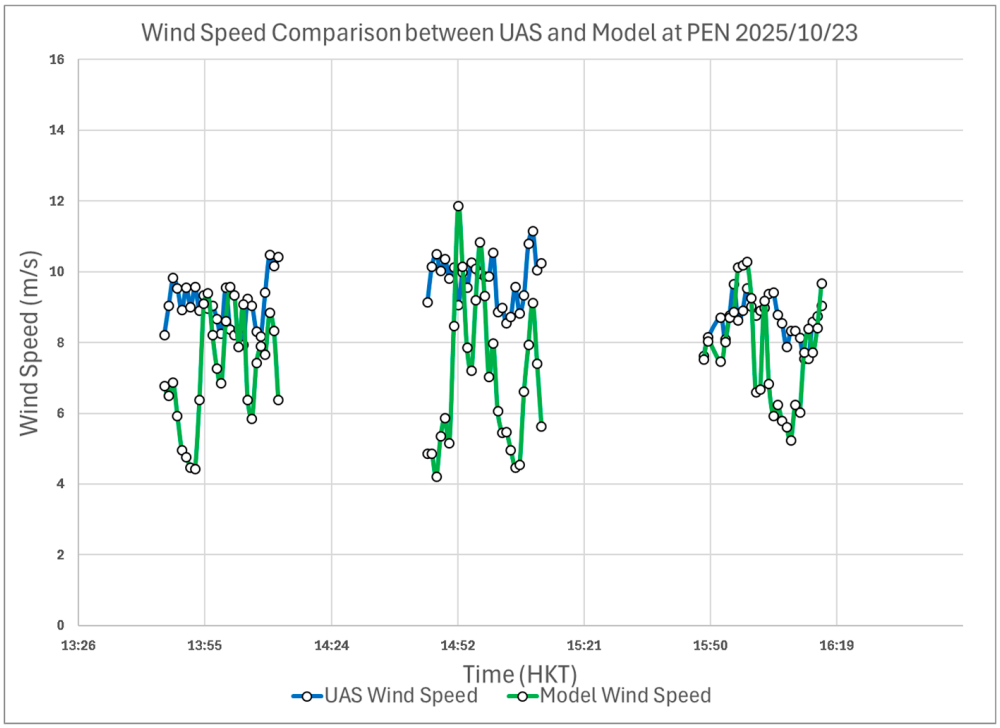


(**c**)

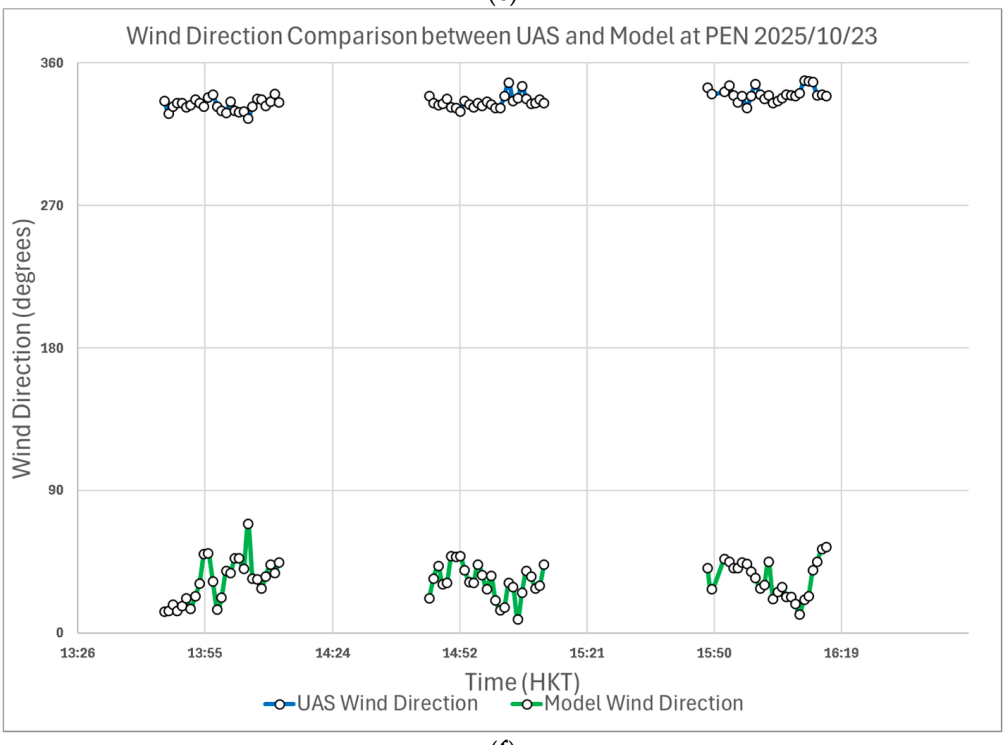


(**d**)

Figure 12. *Cont.*



(**e**)



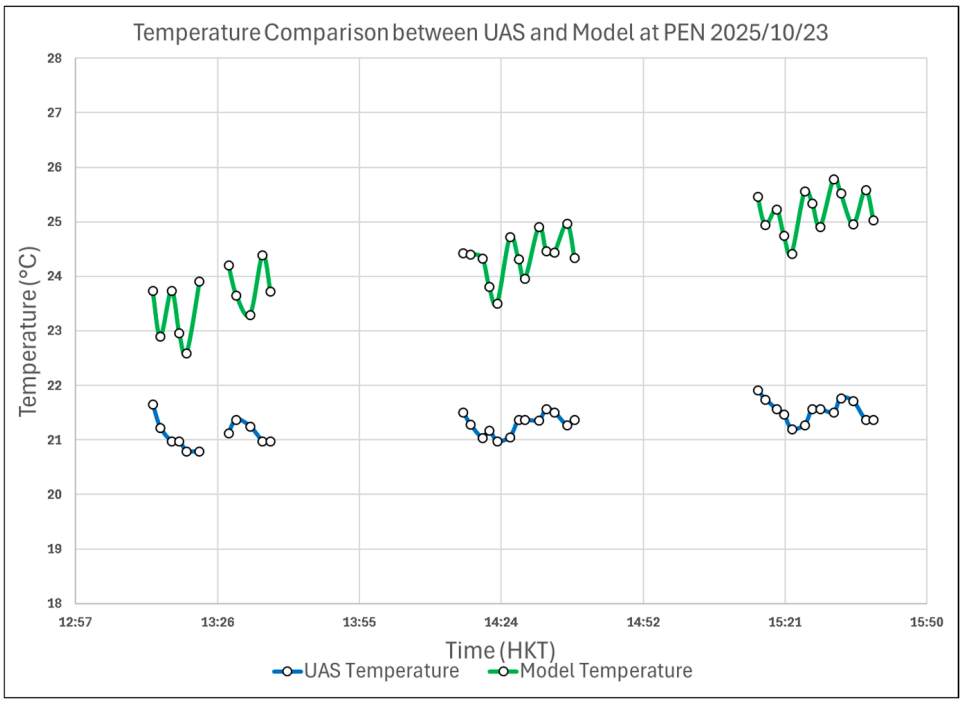
(**f**)

Figure 12. The time series of observed and simulated temperature (**a**), RH (**b**), pressure (**c**), TKE (**d**), wind speed (**e**) and wind direction (**f**) for the round trip flight at Peng Chau.

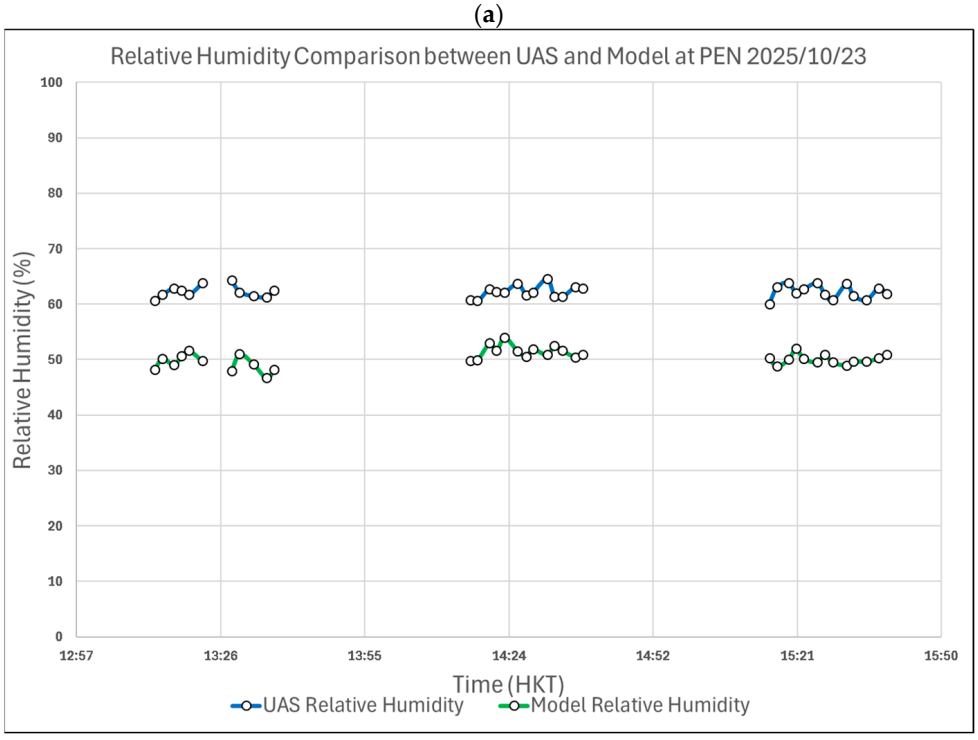
For the vertical profiling flights (time series graphs in Figure 13 and evaluation statistics in Table 5), the correlation is better for the TKE, probably because the simulation manages to catch the generally decreasing TKE with altitude as observed by the UAS measurements. For the wind direction, the simulation again gives too much easterly component.

Table 4. Evaluation statistics of the round trip flight at Peng Chau.

	Temperature (°C)	Relative Humidity (%)	Pressure (hPa)	TKE (m^2/s^2)	Wind Speed (m/s)	Wind Direction (Degrees)
RMSE	3.55	11.48	3.23	0.92	2.68	303.56
Bias	−3.05	11.393	3.17	0.12	1.86	303.27
Correlation	0.55	0.31	0.95	−0.02	−0.01	−0.12

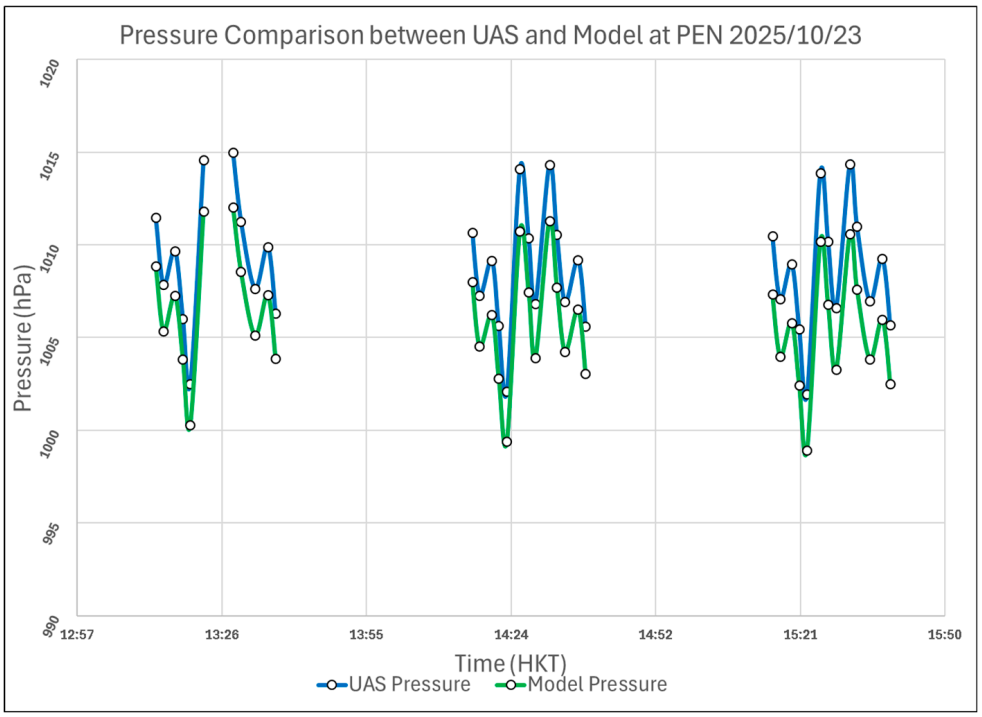


(**a**)

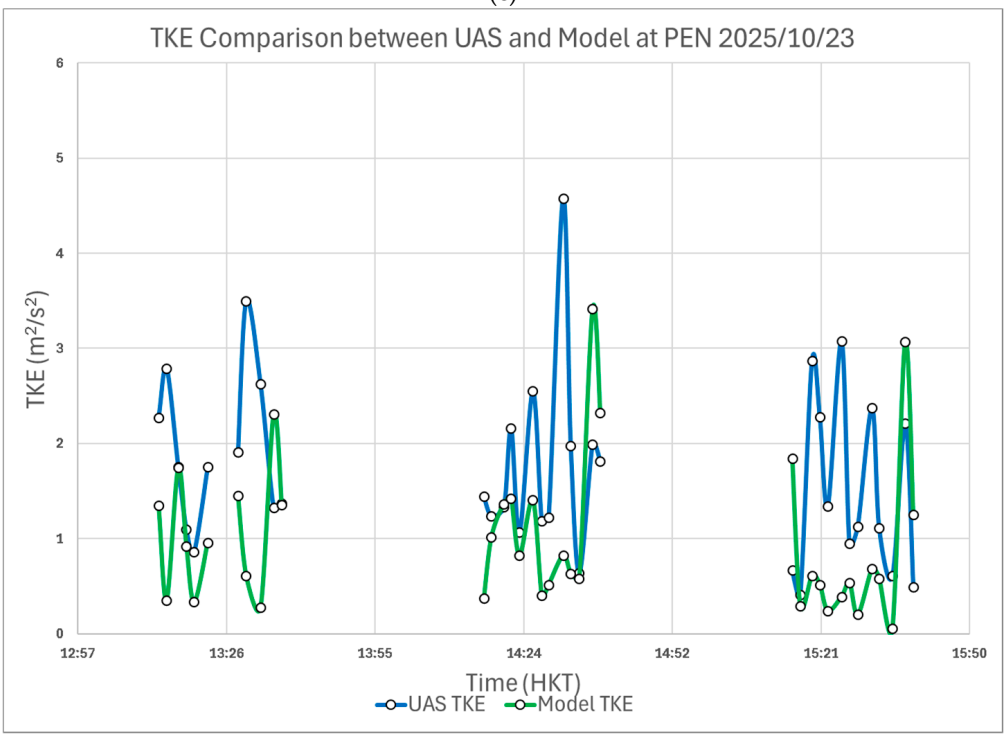


(**b**)

Figure 13. *Cont.*

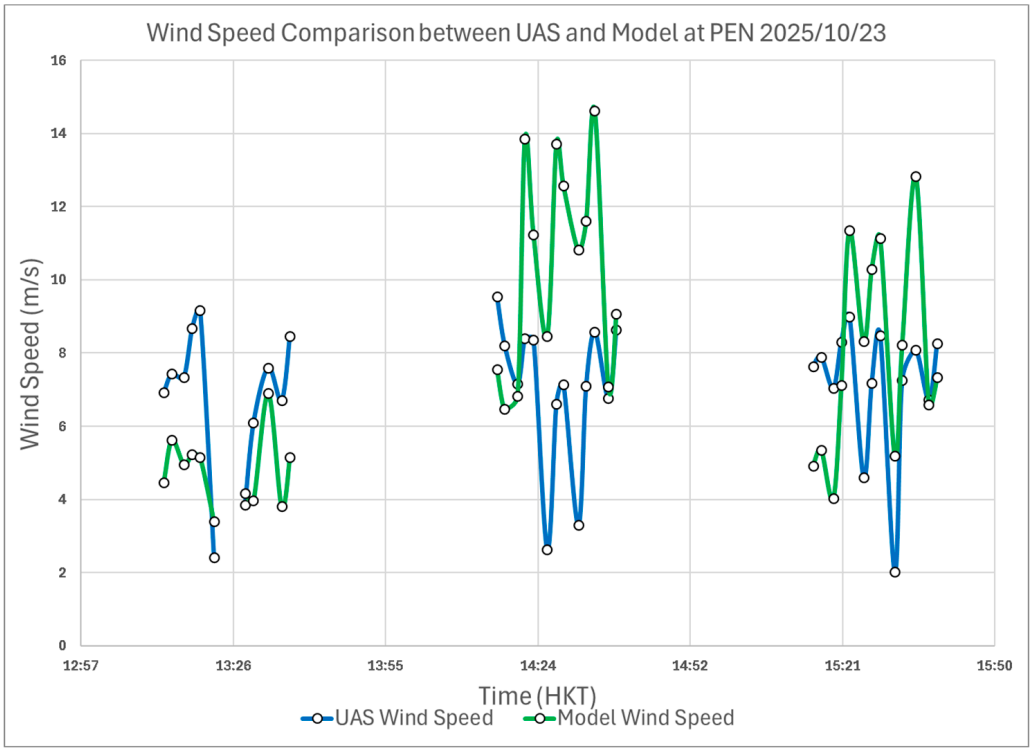


(**c**)

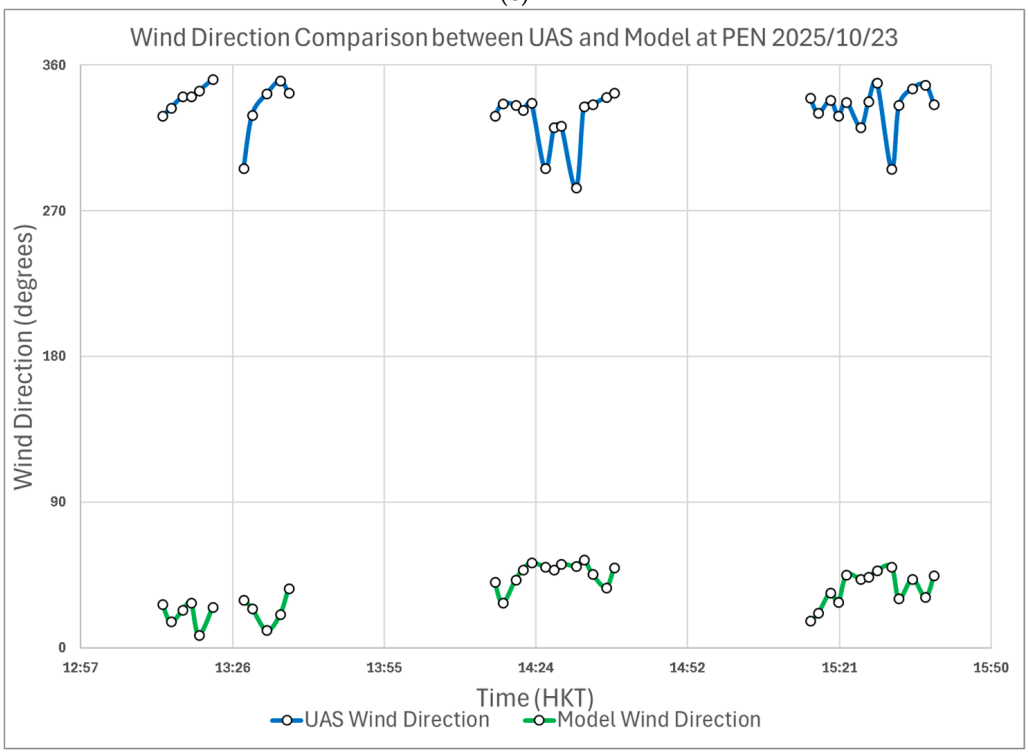


(**d**)

Figure 13. *Cont.*



(**e**)



(**f**)

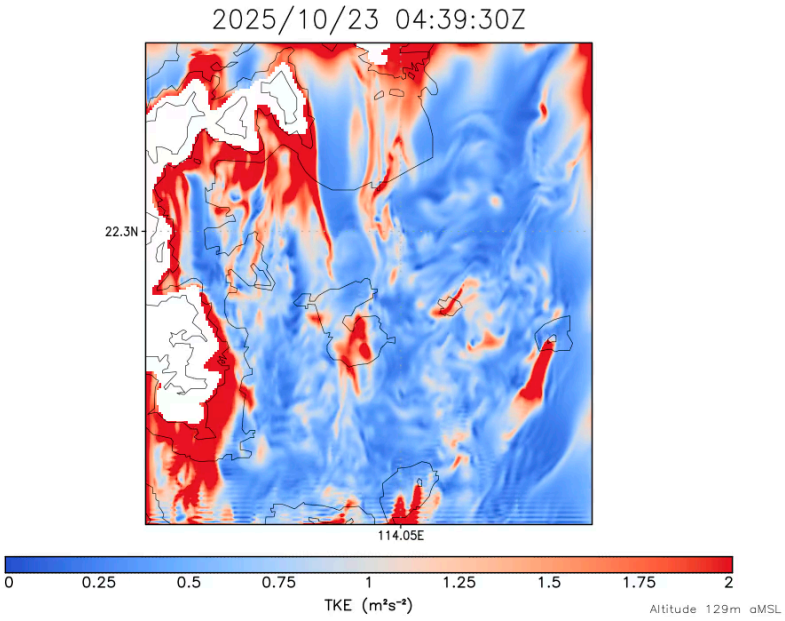
Figure 13. The time series of observed and simulated temperature (**a**), RH (**b**), pressure (**c**), TKE (**d**), wind speed (**e**) and wind direction (**f**) for the vertical profiling flight at Peng Chau.

Sample simulation results of the TKE and wind field at a height of 129 m above sea level over the Peng Chau region are shown in Figure 14. From Figure 14a, higher TKE is found uphill, consistent with the actual observations in Figure 6a. In the northerly winds, upward motion of the airflow is found in the uphill flows in Figure 14b, but there are no direct measurements (e.g., from the UAS) to support the simulated vertical velocity results.

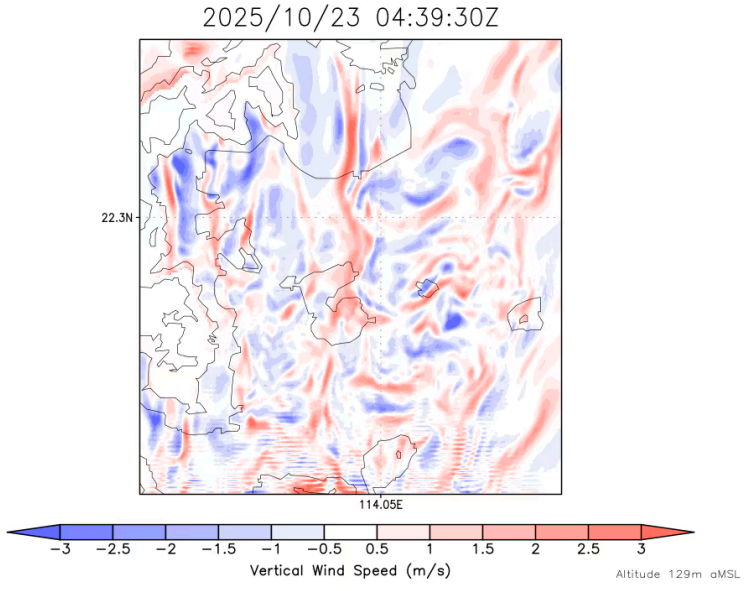
In the earlier part of the simulation, the easterly component of the horizontal wind is still not significant near Peng Chau (Figure 14c) and thus the simulation results have better matching with the actual observations (e.g., wind field in Figure 6a).

Table 5. Evaluation statistics for the vertical profiling flights at Peng Chau.

	Temperature (°C)	Relative Humidity (%)	Pressure (hPa)	TKE (m^2/s^2)	Wind Speed (m/s)	Wind Direction (Degrees)
RMSE	3.15	12.04	2.92	1.37	3.43	297.16
Bias	−3.09	11.90	2.90	0.73	−0.80	296.26
Correlation	0.62	−0.01	0.99	0.06	0.23	−0.35

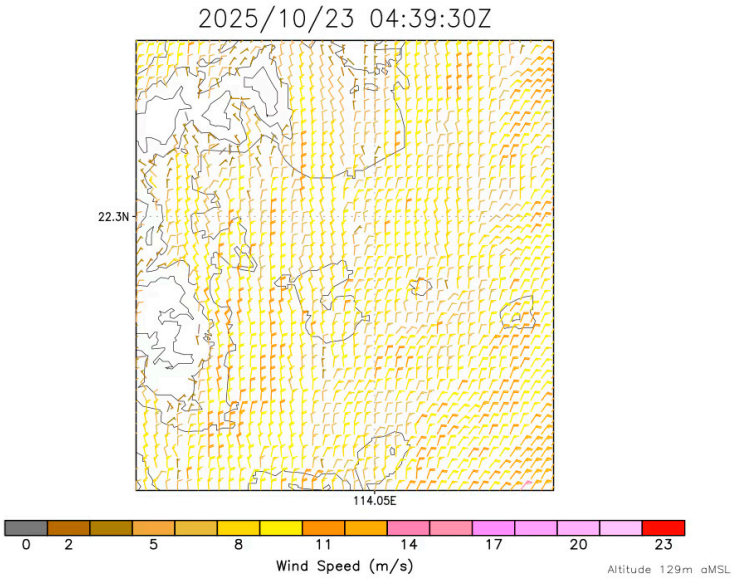


(**a**)



(**b**)

Figure 14. *Cont.*



(**c**)

Figure 14. Simulated TKE (**a**), vertical velocity (**b**) and horizontal wind field (**c**) at a height of 129 m above sea level at Peng Chau.

Based on the simulation results at King's Park and Peng Chau, we have the following observations:

(a) High-resolution NWP modelling is very much affected by the results in the outer domain, so that simulation results for RH and wind direction may not be "corrected" to follow the actual observations more closely even with the use of local terrain data with higher spatial resolution;
(b) Turbulence modelling (in this paper using TKE as the quantity) remains challenging.
(c) The RMSEs are found to be generally of the same order of magnitude as the absolute value itself, though the general decrease in TKE with height is reasonably well captured by the simulation (as shown in the correlation coefficient). This poses a great challenge to the development of a turbulence-alerting service for LAE.
(d) In general, the temperature and pressure simulations are more satisfactory, with good correlation and rather small RMSEs.

5. Discussion

The comparisons between UAS measurements and model forecasts warrant further discussion. As demonstrated in Section 2, comparisons between UAS measurements and ground-based instruments (wind mast, LIDAR, microwave radar) show relatively small discrepancies, with wind speed RMSE meeting the WMO 'breakthrough' level requirement and biases generally small (Figures 3 and 4). This is expected, as both sample the atmosphere at a specific location with comparable temporal resolution. In contrast, comparisons between UAS measurements and NWP model outputs reveal larger differences, particularly for wind direction and turbulent kinetic energy (TKE). Several factors contribute to these discrepancies. First, ground-based and UAS sensors measure atmospheric conditions at discrete points, whereas the NWP model outputs represent grid-averaged values over the finest grid resolution of 40 m. Sub-grid scale turbulence and local flow features cannot be fully resolved, which partly explains why the TKE simulation remains challenging. Second, at King's Park, the urban environment with surrounding buildings and trees introduces flow perturbations that are not fully captured without explicit building data in the model. Finally, time shifts between observed and simulated features are evident in the TKE time

series (Figure 12d), where the model captures similar maximum values but at different times, resulting in low correlation coefficients.

Regarding repeatability of the results, the present study represents an initial case study conducted under autumn northerly wind conditions. Atmospheric boundary layer characteristics can vary significantly with season, synoptic pattern, and local weather regime. For instance, spring-time conditions in Hong Kong often feature stable atmospheric stratification, while summer months are influenced by convective activity and tropical cyclone passages. The NWP model performance observed in this study may differ under these alternative meteorological regimes. Systematic repeatability assessment would require coordinated UAS measurement campaigns across multiple seasons and wind directions, with concurrent NWP simulations to establish model skill scores under diverse conditions. Such multi-period validation is essential before operational deployment of NWP-based turbulence-alerting services for LAE applications.

6. Conclusions

This paper summarizes the results of the comparison between UAS measurements and meteorological equipment measurements, and the evaluation of UAS measurements compared to the simulation results of an NWP model with high spatial resolution. Based on the limited hovering measurements at King's Park, the meteorological data collected by the UAS are found to meet the "breakthrough" level of the WMO requirement. In the vertical profiling flight, the TKE and wind speed appear to be reasonable, at least in line with the expectation of the variation in these quantities with height in an urban environment. Based on this success, a round trip flight and a vertical profiling flight were performed at an actual sandbox project location. This is the first time that detailed meteorological quantities have been collected at this remote island with complex terrain (a bay surrounded by hills). The data collected reveal interesting observations about the vertical profiles of wind speed and TKE, which would form the basis for further investigation of the meteorological conditions of this sandbox location.

The high-resolution NWP simulation successfully applied to HKIA has been found to have mixed results for the simulations of the weather conditions at King's Park and Peng Chau. Although it manages to capture some general features, such as the decrease in TKE with height and the variation in wind speed, simulation of the time evolution of TKE remains challenging and wind direction simulation results are still very much affected by the outer model, with minimal correction even with the input of local terrain data. Further work would be conducted in this regard: (a) the inclusion of building information for King's Park simulation in order to better represent the urban environment, and (b) the assimilation of local observations so that some degree of "correction" could be achieved to the outputs of the outer model. Moreover, local turbulence data such as measurements by a vertically profiling LIDAR could be assimilated in order to better forecast the future evolution of TKE or eddy dissipation rate (EDR), at least the turbulence encountered during the flight of the UAS (in the next couple of hours) could be nowcast.

Moreover, establishing the repeatability of these findings across different seasons, synoptic patterns, and atmospheric stability regimes remains an important objective for future work. The current results should be interpreted as initial validation under autumn northerly wind conditions, with multi-season campaigns required to establish model performance across the full range of meteorological scenarios encountered in Hong Kong. Ultimately, more measurements of UAS would then be evaluated, with NWP simulations to be performed, to better understand the atmospheric characteristics in more diverse meteorological situations.

Author Contributions: Conceptualization, P.W.C.; Methodology, W.H.L. and P.W.C.; Software, M.C.L., K.K.L. and P.W.C.; Validation, W.H.L. and M.C.L.; Formal analysis, W.H.L. and M.C.L.; Investigation, M.C.L.; Resources, K.K.L.; Writing—original draft, P.W.C. All authors have read and agreed to the published version of the manuscript.

Funding: This research received no external funding.

Institutional Review Board Statement: Not applicable.

Informed Consent Statement: Not applicable.

Data Availability Statement: The raw data supporting the conclusions of this article will be made available by the authors on request.

Conflicts of Interest: The authors declare no conflict of interest.

References

1. Barbieri, L.; Kral, S.T.; Bailey, S.C.C.; Frazier, A.E.; Jacob, J.D.; Reuder, J.; Brus, D.; Chilson, P.B.; Crick, C.; Detweiler, C.; et al. Intercomparison of small unmanned aircraft system (sUAS) measurements for atmospheric science during the LAPSE-RATE campaign. *Sensors* **2019**, *19*, 2179. [CrossRef] [PubMed]
2. Lin, L. Study on the synergistic development of the drone industry and low-altitude economy. *J. Glob. Humanit. Soc. Sci.* **2024**, *5*, 328–333. [CrossRef]
3. Transport and Logistics Bureau. Highlights—Transport. 2024. Available online: https://www.tlb.gov.hk/eng/highlights/transport/low-altitude.html (accessed on 13 February 2026).
4. Greene, B.R.; Otterstatter, L.M.; Salesky, S.T. How Representative Are Uncrewed Aircraft System Measurements of the Convective Boundary Layer? *Geophys. Res. Lett.* **2025**, *52*, e2024GL114291. [CrossRef]
5. Lam, M.C.; Leung, W.H.; Lo, K.W.; Lai, K.K.; Chan, P.W.; He, J.Y.; Li, Q.S. A Pilot Study on Meteorological Support for the Low-Altitude Economy—Consistency of Meteorological Measurements on UAS with Numerical Simulation Results. *Atmosphere* **2026**, *17*, 107. [CrossRef]
6. de Boer, G.; Butterworth, B.J.; Elston, J.S.; Houston, A.; Pillar-Little, E.; Argrow, B.; Bell, T.M.; Chilson, P.; Choate, C.; Greene, B.R.; et al. Evaluation and intercomparison of small uncrewed aircraft systems used for atmospheric research. *J. Atmos. Ocean. Technol.* **2024**, *41*, 127–145. [CrossRef]
7. Lo, K.W.; Chan, P.W.; Lai, K.K.; Lau, S.P.W.; Zhao, Z.H. Case studies of the winds in the urban area of Hong Kong–Microclimate station observations and high resolution numerical simulations. *Heliyon* **2024**, *10*, e37865. [CrossRef] [PubMed]
8. World Meteorological Organization (WMO) OSCAR. The Repository of Requirements for Observation of Physical Variables (Definitions of Threshold, Breakthrough, Goal). Available online: https://space.oscar.wmo.int/observingrequirements (accessed on 3 March 2026).
9. Stull, R.B. *An Introduction to Boundary Layer Meteorology*; Kluwer Academic Publishers: Dordrecht, The Netherlands, 1988. [CrossRef]
10. Kaimal, J.C.; Finnigan, J.J. *Atmospheric Boundary Layer Flows: Their Structure and Measurement*; Oxford University Press: New York, NY, USA, 1994. [CrossRef]
11. Wyngaard, J.C. *Turbulence in the Atmosphere*; Cambridge University Press: Cambridge, UK, 2010.
12. Dyer, A.J. A review of flux–profile relationships. *Bound. Layer Meteorol.* **1974**, *7*, 363–372. [CrossRef]
13. Wieringa, J. Updating the Davenport roughness classification. *J. Wind. Eng. Ind. Aerodyn.* **1992**, *41*, 357–368. [CrossRef]
14. Hlywiak, J.; Singh, J.; Ruiz-Plancarte, J.; Flagg, D.D.; Yamaguchi, R.; Ortiz-Suslow, D.G.; Doyle, J.D.; Wang, Q.; Hong, X.; Shen, L. A Simple Parameterization for the Inland Coastal Aerodynamic Roughness Length within Onshore Flows. *Bound. Layer Meteorol.* **2026**, *192*, 12. [CrossRef]
15. Cooke, J.; Jerolmack, D.; Park, G.I. Mesoscale structure of the atmospheric boundary layer across a natural roughness transition. *Proc. Natl. Acad. Sci. USA* **2024**, *121*, e2320216121. [CrossRef] [PubMed]
16. Pielke, R.A.; Cotton, W.R.; Walko, R.L.; Tremback, C.J.; Lyons, W.A.; Grasso, L.D.; Nicholls, M.E.; Moran, M.D.; Wesley, D.A.; Lee, T.J.; et al. A comprehensive meteorological modeling system—RAMS. *Meteorol. Atmos. Phys.* **1992**, *49*, 69–91. [CrossRef]
17. *RAMS Model*, v6.3.04. Official Software Release. Zenodo: Geneva, Switzerland, 2023. [CrossRef]
18. Shi, Y.; Tao, T.; Wu, H.; Chen, Y.-R.; Han, Z.; Zhou, D.; Chen, W.-L.; Cao, Y. Assessment of turbulence model effects on WRF-LES of separated turbulent flows past a 3D hill. *J. Wind. Eng. Ind. Aerodyn.* **2024**, *254*, 105910. [CrossRef]
19. Joshi, P.; Lin, T.S.; He, C.; Lamer, K. Urban weather modeling using WRF: Linking physical assumptions, code implementation, and observational needs. *Geosci. Model Dev.* **2025**, *18*, 7869–7890. [CrossRef]

20. Smagorinsky, J. General circulation experiments with the primitive equations. Part I: The basic experiment. *Mon. Weather. Rev.* **1963**, *91*, 99–164. [CrossRef]
21. Deardorff, J.W. Stratocumulus-capped mixed layers derived from a three-dimensional model. *Bound. Layer Meteorol.* **1980**, *18*, 495–527. [CrossRef]
22. Chan, P.W.; Lai, K.K.; Li, Q.S. High-resolution (40 m) simulation of a severe case of low-level windshear at the Hong Kong International Airport—Comparison with observations and skills in windshear alerting. *Meteorol. Appl.* **2021**, *28*, e2020. [CrossRef]

Disclaimer/Publisher's Note: The statements, opinions and data contained in all publications are solely those of the individual author(s) and contributor(s) and not of MDPI and/or the editor(s). MDPI and/or the editor(s) disclaim responsibility for any injury to people or property resulting from any ideas, methods, instructions or products referred to in the content.